Author's response

We would like to thank the three referees for their detailed and constructive comments. The referee comments are quoted below (shown in italics) and our responses are shown with the plain text. Changes to the manuscript are also shown after our responses when the changes cover a specific part of the manuscript; all changes are shown in the marked-up manuscript (deleted text is shown with red strike through font and new text is indicated with blue color). The updated manuscript has also two completely new figures (Figs 5 and 7) and Fig. 3 is updated.

D. Baumgardner (Referee)

There are a number of issues that I have annotated in the manuscript (Summary material), some that I list here, that are related to clarity of understanding in the manuscript, as well as interpretation of the results. These are listed here in the order they were annotated in the manuscript. The annotated manuscript also contains my minor edits where I have tried to provide suggestions for better readability.

Reply: We have made several updates to the manuscript based on the annotated manuscript.

Changes to the manuscript: Several - please see the marked up manuscript.

Major issue 1 I am making a very strong recommendation that the term "coating" either be completely removed when discussing the mixing state of particles or be clearly defined, something like Schwarz et al. have used in their publications. I have had a discussion with Dr. Schwarz on this matter (personal communication) and he has emailed me the following response to my question about his opinion about the use of the term "coating":

"In my papers, I always have a sentence that reads like "the materials internally mixed with BC (here referred to generically as "coatings" without implying any knowledge of morphology)".

There can certainly be chemical processes whereby inorganic or organic material might condense or be deposited on the surfaces of the elemental carbon particles during the aging processes, but it is just as likely that during the aging process coagulation is also occurring between the rBC and other non-refractory material. For example in the abstract, describing a "coated to core diameter of 2", suggests a particle consisting of a solid core and a shell. This might actually describe a very small fraction of the particles but is unrealistic based upon the multitude of microscopic analyses that would suggest that the morphology of these particles is much more complicated. As an author of several SP2 papers I am guilty of propagating this same concept that I would now like to try and change in terminology. Instead of referring to "coated" rbC, I think the more accurate and correct would be "Internally mixed" rBC, since the authors have already defined in their opening discussion the term "internally mixed" to mean non-refractory material mixed with refractory material. I would also be willing to accept an acronym for this type of material, e.g. IMrBC. The derivation of the fraction of mixing remains the same. Instead of referring to a "coating layer" you would change it to "mixed fraction" so that in the abstract, "coated to core diameter of 2" would become "Total mixed to core diameter ratio of 2". Note that Huang et al (2012) avoid the term "coated" and instead use "Internally mixed". The same should be done in this paper.

Reply:
We agree that the structure of the BC-containing particles is unlikely as simple as ex pected by the core-shell model. Therefore, we will also avoid term "coated". However, the replacement term "internally mixed rBC" can have different meanings for a single particle (is it not pure rBC, but mixed with other species) and for aerosol populations (all particles are containing rBC so that there are no rBC-free particles), which is the definition used in the manuscript. For clarity, we will continue to use terms external and internal mixing when referring to aerosol populations. For a single particle containing both rBC and non-absorbing material we will use term "mixed" (or similar depending on the context) instead of "coated".

Regarding the parameter describing rBC content in a single particle, term "mixed fraction" is unambiguous as it could refer to particle populations or single particles. Although rBC volume fraction would be independent of morphology, its magnitude (about 0.01) is not as convenient as that of the diameter ratio and the diameter ratio seems to be better for averaging (volume ratio depends more on particle size). So, we will express rBC content as "particle diameter to rBC core volume equivalent diameter ratio" (briefly: particle to rBC core diameter ratio). This is neutral in the sense that it does not expect any morphology for rBC. Also, particle diameter is the standard term for particle size. Clearly, the terminology needs to be clarified, but this is not the purpose of our paper.

Changes to the manuscript: Several - please see the marked up manuscript.

Major Issue 2

The authors have tried to describe the operating principles of the SP-2 and analysis of the scattering and incandescence signals in their own words but in doing so have incorrectly described a number of the fundamental aspects. One example, on page 15627: "Nonabsorbing particles scatter laser light so that the maximum scattering signal is proportional to the scattering cross section of the particle, which is calculated using the Mie approximation..".

This is misleading since it suggests that only those particles without rBC are used for sizing. Here and in a previous statement the authors suggest that only non-rBC scatter light but this is obviously not true. I have noted in my annotated version all the places where there are inaccuracies; however, I would suggest that the authors only present the minimum that is needed to explain the operation of the SP-2 and how the basic parameters are derived. That includes removing the lengthy discussion on the LEO derivation of size. It is sufficient to state that the size is derived from the scattering signal using the leading edge technique described by Gao et al. Then the mixing fraction can be simply described as the ratio of the rBC mass diameter to the mixed particle equivalent optical diameter without the need for a lengthy justification since this is what other studies have already published.

Reply:
We have clarified this based on the referee comments in the annotated version of the manuscript. The description of the SP2 and data analysis is also significantly shortened (e.g. the LEO part is almost completely removed).

Changes to the manuscript: Several - please see the marked up manuscript (pages 6 and 7).

Major Issue 3

There are no uncertainties discussed for the SP2, MAAP or Aethalometer. This is a serious omission. Given the uncertainties in deriving the mixing fraction because of the assumed refractive index and particle density, as well as the possibly very large uncertainties in deriving the eBC from filter based techniques, anytime quantitative comparisons are being made between measurements being made by different instruments or techniques, these have to be given in the context of the expected variations.

Secondly, the operating principles of the filter-based instruments need to be included in the instrumentation section. Briefly, with adequate references, just as with the SP2.

Reply:
We have added some discussion about the uncertainties. Some of the uncertainties are also discussed in Sect. 3.4, where SP2 and optical black carbon measurements are being compared. The filter based instruments have now more references to publications where their operation and uncertainties are fully described. More details are given about the SP2, because MAAP and Aethalometer are routinely used instruments and this study is heavily focused on the SP2 measurements.

Changes to the manuscript: Several - please see the marked up manuscript (pages 5-7).

Major issue 4

The analysis of the variations in the rBC parameters is cursory at best. The correlation with CO is interesting but the trajectory analysis fall short of providing much in the way of useful information on the history of the rBC prior to its arrival at the research site. In figure 4 I am assuming that the origin is being determined from the point where the air mass was 5 days previously but there is a very wide range of values in each of the sectors, particularly the one labeled continental Europe. This suggests that there is a lot more going on to drive the variations than just where the air was 5 days previously. Here are some of the questions that need to be addressed:

1) How far has the air traveled in 5 days along its trajectory and how does that relate to the three most important parameters – rBC mass, number fraction and mixing state? 2) From what altitude is the air coming, i.e. has it been near the surface most of the 5 days or has it descended from a higher altitude? How does this impact the three parameter? 3) How does the rBC to eBC ratio vary with the rBC/CO and eBC to CO ratios? If the overestimate of eBC by the filter methods is due to absorbing material that is not rBC, then this is likely seen in the air mass history. 4) What is the correlation between mixing state and rBC mass, mixing state and number fraction and mixing state and rBC/CO? These are all possible clues to the aging processes.

Reply:
Figure 4 shows the average direction and distance, which is not the same as those of the first trajectory coordinate point. Different trajectory parameters (also trajectory length and altitude (question 2), which did not show any correlation with the rBC parameters) were tested and the two parameters (described in section 2.3) were selected, because they have the best correlations with the rBC parameters. It is also clear that the trajectories cannot explain variations in rBC mixing state (question 1). This is now clarified.

Linear fit to eBC as a function of CO gives a slope of 4.35 ng m^{-3} ppb^{-1}, which is slightly higher than expected (ideally, should be five times that for rBC). Likewise, rBC/eBC to rBC/CO is about the same as rBC/eBC, which is about 0.2. As mentioned in the text, air mass history described by trajectories had no apparent

effect on rBC properties except mass concentration, and therefore cannot explain the low rBC to eBC ratio. Furthermore, the ratio is more or less constant although air masses are not, so air mass history cannot explain the difference between eBC and rBC.

Regarding question 4, we have calculated all cross correlations between the mixing state parameters, but nothing relevant was found. This is also evident from Fig. 3. We have also tried to find explanations for rBC/CO, but nothing relevant was found. This will be clarified.

Changes to the manuscript: Several - please see the marked up manuscript (Sects 2.3, 3.3 and 3.4).

Other Comments

Figure 2 should include the average size distribution from the SMPS. It is stated that there are significant numbers of particles below 75 nm from Fig. 2 but this is speculation without also showing the SMPS distribution that should go down to as small at least as 10 nm.

Reply:
We will clarify that the rBC core diameters (not particle diameters measured by the DMPS) are often smaller than 75 nm. This can be seen from the rBC core number size distribution, which have maximum at the 75 nm detection limit. The other reason for not including DMPS size distributions to figure 2, is that both size (rBC core vs particle) and number (rBC-containing vs all particles) scales are different. We have now given a reference to previous studies from Pallas where DMPS size distributions are shown.

Changes to the manuscript:
Line 132: "Since the weather station data is largely missing, in cloud time periods are found by comparing particle number size distributions from two Differential Mobility Particle Sizers (DMPS; see Hatakka et al. (2003) or Komppula et al. (2005) for the description of the measurement setup and instruments)."
Line 295: "Figure 2 shows campaign averages of rBC mass and number size distributions. ~~The~~ (shown as a function of rBC core volume equivalent diameter). The peak of the number size distribution ~~extends well below~~ seem to be unresolvable due to the 75 nm detection limit, which means that distribution parameters (total number, mode and width) cannot be calculated or determined from a fit to the data."

Page 15626, line 10, "The SP2 was connected to the PM10 sample line, which means that some ice nuclei (IN) and cloud condensation nuclei (CCN) are not detectable when the station is covered by clouds." And again on page 15631, line 25, "As explained in Sect. 2.2, SP2 measurements can be biased during the in cloud time periods, because some ice and cloud condensation nuclei become too large to be detected". I don't understand what this means. The presence of CCN and IN have nothing to do with the presence of clouds so these statements are incorrect.

Reply:
The statements mean that when the station is covered by clouds, cloud and ice particles larger than 10 microns are removed by the PM10 inlet. This means that those particles that have been forming these clouds (IN and CCN) are not detected by the SP2. We have clarified this part of the text by removing terms IN and CCN.

Changes to the manuscript:
Section 2.2: Several - please see the marked up manuscript.
Line 312: "As explained in Sect. 2.2, SP2 measurements can be biased during the in cloud time periods, because ~~some ice and cloud condensation nuclei become too large to be detected~~ most activated particles are removed by the inlet system."

In addition to figure 3 time series, since it is mentioned that there is a correlation between the rBC mass and the wind direction and CO, these parameters should be included in the time series.

Reply: We have added trajectory directions (better than wind direction) and CO time series to Fig. 3.

Changes to the manuscript: Please see updated Fig. 3.

The rBC mass concentration is correlated with CO, and a correlation coefficient and slope given. Please show a figure with these data. These are numbers that can be compared to correlations that have been published elsewhere, i.e. Han et al (2009), Zhou et al (2009), Andreae et al. (2006), Kondo et al (2006), Chou et al (2010), Spackman et al (2008), Baumgardner et al (2002). The BC/CO ratios range anywhere from 1 – 10 ug/m3 BC to 1 ppm of CO.

Reply:
We have added a figure showing the correlation. We know that there are several papers published on this topic, and this is why we already had five references. The references in the paper were selected so that they are based on SP2 data and rBC (slopes could be different for eBC), but it seems that from the references given above the first five and the last are not related to SP2 measurements. However, reference to Spackman et al (2008) has been added. The selected references show that the smallest BC/CO ratios are typically larger than 1 ngm^{-3} ppb^{-1}, which is already higher than our value.

Changes to the manuscript: Please see Fig. 4 and updated text (lines 400-426).

Please also note the supplement to this comment: http://www.atmos-chem-physdiscuss.net/15/C4720/2015/acpd-15-C4720-2015-supplement.pdf

Reply: The manuscript has been updated based on these comments.

Changes to the manuscript: Several - please see the marked up manuscript.

Anonymous Referee #3

General comments:

1. The reason at the root of the discrepancy between the aethalometer and MAAP with respect to the SP2 is not clear. The explanations in the paper are not too convincing to me; therefore, it is difficult to assess the goodness of the estimation of the LAC volume fraction used at the end of the paper. Most aethalometers have multiple wavelengths, some of the proposed ideas for why the SP2 and the aethalometer do not agree could be tested using the information provided at the different wavelengths, for example through the Angstrom exponent. Could it be that the mass density chosen for rBC plays also a role into these discrepancies? Finally, it might help to discuss some papers that already reported issues with filter-based instrumentation such as those by Cappa et al., Lack et al. and Subramanian et al. (1. Bias in Filter-Based Aerosol Light Absorption Measurements Due to Organic Aerosol Loading: Evidence from Laboratory Measurements, Christopher D. Cappa , Daniel A. Lack , James B. Burkholder , A. R. Ravishankara, Aerosol Science and Technology Vol. 42, Iss. 12, 2008; 2. Bias in Filter-Based Aerosol Light Absorption Measurements Due to Organic Aerosol Loading Evidence from Ambient Measurements, Daniel A. Lack , Christopher D.

Cappa , David S. Covert , Tahllee Baynard , Paola Massoli , Berko Sierau , Timothy S. Bates , Patricia K. Quinn , Edward R. Lovejoy , A. R. Ravishankara, Aerosol Science and Technology, Vol. 42, Iss. 12, 2008; Yellow Beads and Missing Particles: Trouble Ahead for Filter-Based Absorption Measurements, R. Subramanian , Christoph A. Roden , Poonam Boparai , Tami C. Bond, Aerosol Science and Technology, Vol. 41, Iss. 6, 2007)

Reply:

We do not have complete explanation for the difference between Aethalometer/MAAP and SP2. We have modified this section so that instrument bias (due to inaccurate instrument parameters) is one potential explanation and the presence of light absorbing material that cannot be detected by the SP2 is the other explanation. It is clear that the instrument and other parameters (including mass density of rBC) have some uncertainties, but we are using the best available information, which means that the results are as accurate as they can be. We have calculated the Ångström exponent from the Aethalometer data and found nothing exceptional; the exponent is close to 1.2, which indicates relatively weak wavelength dependency. This is now mentioned in the paper.

Changes to the manuscript: Several - please see the marked up manuscript (especially Sects 2.2 and 3.4).

2. An abundant body of literature on single particle microscopy and single particle numerical calculations of the optical properties of rBC mixed with other material and the effects this mixing might have on radiative forcing has been ignored. Including a discussion of some of this literature might improve the discussion of the results found by the authors and the relevance of the paper.

Reply:

In the introduction we have added a reference to the Bond et al. (J. Geophys. Res., 118, 5380-5552, 2013) review, which summarizes several single particle microscopy studies and studies examining the effect of mixing state on aerosol radiative properties. We have also clarified our aim, which is to compare different mixing representations based on the new information about the mixing state and concentrations from the SP2 and MAAP measurements. To our knowledge, there are no similar studies that could be directly compared with our study.

Changes to the manuscript:

Line 52: "Individual ~~particles can also have different structures such~~ absorbing particles have wide range of structures starting from small spherules which form chain-like aggregates and usually end up being densely packed clusters mixed with non-absorbing material (e.g. Bond et al., 2013). Typical radiative transfer models describe these as bare or coated black carbon ~~particle~~ particles or a homogenous mixture of black carbon and non-absorbing compounds."

Line 504: "Several studies have been using numerical models to quantify the effects of black carbon mixing state on aerosol radiative properties and climate (e.g. Bond and Bergstrom, 2006; Adachi et al., 2010; Bond et al., 2013), however, most of these studies are made without detailed experimental information about the mixing state that can be obtained from single particle instruments such as the SP2."

Line 521: "Particle structures cannot be directly measured by the SP2, but single particle imaging studies have shown that aged ambient particles are typically composed of a compact black carbon cluster mixed with non-absorbing material, which is often described by a homogenous particle or a coated black carbon core model (e.g. Bond et al., 2013)."

Specific comments:

Abstract:

1. "SP2 is a unique instrument that can give..." several instrument might be considered "unique". I would suggest to just write "SP2 provides..."

Reply: Done.

Changes to the manuscript:
Line 4: "The SP2 ~~is a unique instrument that can give~~ provides detailed information about…"

2. I suggest removing "As expected"

Reply: Done.

Changes to the manuscript:
Line 6: "~~As expected, the~~ The measurements showed…"

3. "...the number fraction of particles containing rBC..." this value is calculated only in the range of sizes detected by the SP2? Maybe it should be noted here.

Reply: The size range is now given.

Changes to the manuscript:
Line 8: "The rBC mass was log-normally ~~distributed rBC core size was relatively constant with an average geometric~~ distributed showing a relatively constant rBC core mass mean diameter with an average of 194 nm (75–655 nm sizing range). On the average, the number fraction of particles containing rBC was 0.24 (integrated over 350–450 nm particle diameter range) and the average ~~rBC core size in these particles was half of the total size (coated to core~~ particle diameter to rBC core volume equivalent diameter ratio was 2.0 (averaged over particles with 150–200 nm rBC core volume equivalent diameters)."

4. "Comparison of the measured rBC mass concentration with that of the optically detected equivalent black carbon (eBC)..." add "...using an aethalometer and a MAAP"

Reply: Done.

Changes to the manuscript:
Line 18: "…detected equivalent black carbon (eBC) ~~showed~~ using an Aethalometer and a MAAP showed that eBC was larger by a factor…"

5. I think that the sentence "(separate non-absorbing and coated rBC particles)" is not very clear here until one reads the rest of the paper, so my suggestion is to just remove this. If the authors prefer to keep it, they might want to explain it a bit more.

Reply: We have now removed the sentence.

Changes to the manuscript:
Line 24: "…mixing state ~~(separate non-absorbing and coated rBC particles)~~ means…"

Introduction:

- Line 39: "For example, it can be distributed" what "it" refers to might be confusing, I suggest to specify.

Reply: We have now clarified that it refers to absorbing material.

Changes to the manuscript:
Line 48: "…For example, ~~it~~ the absorbing material can be distributed so that a large fraction…"

- Lines 41-42: "By definition, an aerosol population is externally mixed when not all particles are absorbing and internally mixed when all particles are absorbing." This could be confusing as an externally mixed population of particles could be just made of non-absorbing aerosols at all, just with different composition. I think it should be clarified that this refers to absorbing aerosols only.

Reply: We have now clarified that this is an optical definition.

Changes to the manuscript:
Line 50: "~~By definition~~ From the optical point of view, an aerosol…"

- Lines 56-57: "This means that non-refractory absorbing material such as brown carbon cannot be detected by the SP2." I would think another main reason the SP2 would not detect directly brown carbon is that it operates with a NIR laser at a wavelength where brown carbon would not absorb.

Reply: This wavelength limitation is now mentioned.

Changes to the manuscript:
Line 70: "~~This means that non-refractory absorbing material such as brown carbon cannot be detected by the SP2.~~"
Line 472: "Since brown carbon is typically non-refractory and weakly absorbing at the near-infrared wavelengths, it cannot be detected by the SP2."

Experimental:

- Lines 97-98: I think that at this point in the paper, this sentence is not clear, what is meant becomes clearer later on, but it might be good to either remove or clarify this sentence here. In general I found all this paragraph until line 106 confusing and unclear. I would suggest clarify it a little bit more maybe by adding some details.

Reply: We have now clarified this paragraph.

Changes to the manuscript: Several - please see the updated Sect. 2.2.

- Line 107: Specify the model of the aethalometer. Is this the 7-wavelength model? In general provide model and maker also for the other instruments such as MAAP, aethalometer, DMPS and gases.

Reply: Done.

Changes to the manuscript: Several - please see the updated Sect. 2.2.

- Lines 122-123: The particles actually pass through the laser cavity.

Reply: Fixed.

Changes to the manuscript:
Line 169: "Briefly, sample aerosol particles travel through a ~~powerful laser beam, where non-absorbing and absorbing particles are identified based on the scattered laser light and emissions of~~ laser cavity (1064 nm wavelength), where absorbing"

- Line 123: "...absorbing particles are identified..." not all absorbing particles, but mostly rBC. For example, brown carbon is probably not detected.

Reply: This part of the text is updated.

Changes to the manuscript:

Line 169: "Briefly, sample aerosol particles travel through a ~~powerful laser beam, where non-absorbing and absorbing particles are identified based on the scattered laser light and emissions of~~ laser cavity (1064 nm wavelength), where absorbing refractory particles are quickly heated to a temperature where they emit visible light (laser-induced incandescence)~~, respectively~~."

Results:

- Line 194: "Ambient temperature..." is this the daily average, the min the max, something else?

Reply: It is hourly average, which is now mentioned in the text.

Changes to the manuscript:

Line 285: "Ambient temperature was initially about -2°C (hourly averages), but decreased…"

- Line 226: "number fraction of particles containing rBC is 0.24..." as for the abstract, please define clearly the size range used for this calculation.

Reply:

We have now added size ranged to the previous paragraph where the parameter time series (shown in Fig. 3) are described.

Changes to the manuscript:

Line 306: "Figure 3 shows the time series of the main rBC properties including the total mass concentration (c_{rBC})~~,~~ and geometric mass mean diameter (GMD_{rBC}) for the 75–655 nm rBC core diameter detection range, number fraction of particles containing rBC (N_{rBC}/N_{total}; calculated using 350–450 nm particle size range), and ~~coated to~~ particle to rBC core diameter ratio (D_p/D_{rBC}; calculated using 150–200 nm rBC core size range)."

- Line 309: Please explain how the Δ are calculated, in other words, how is the reference value estimated? In addition, it might be interesting to provide also the slopes for the other gases.

Reply:

We have now explained the fit and the calculation of the reference value. Since our focus is on rBC mixing state, we have shown only carbon monoxide (CO) which is the most commonly used tracer gas. Giving the other slopes would require proper description, interpretation and comparison with literature values; this would make this section too long.

Changes to the manuscript:

Line 407: "Pearson's correlation coefficient for ~~a linear fit between rBC and CO~~ the fit is 0.74, slope $\Delta rBC/\Delta CO$ is 0.742 ng m^{-3} ppb^{-1} (ppb=nmol mol^{-1}) and the offset is -93 ng m^{-3}. Solving the background CO concentration (CO concentration where rBC concentration is zero) ~~is~~ from the fitted slope and offset gives 126 ppb."

- Lines 329-331: it might be interesting to look at the ΔrBC/ΔCO versus distance from the source as given by the hysplit.

Reply:

Note that ΔrBC/ΔCO is a single value calculated from the campaign data. However, we have examined if the deviation of the individual data points from the linear fit depends on the HYSPLIT parameters, but clear dependencies were not found.

Changes to the manuscript:

Line 421: "As can be seen from Fig. 4, the values cover a relatively wide range around the linear fit. This variability does not show clear dependence on the available trajectory, meteorological or rBC mixing state parameters. As an example, the marker color shows the particle to rBC core diameter ratio for each data point. Although the higher diameter ratios seem to be mostly above the linear fit, these are not clearly separated from the other data points."

- Line 352: That's true but MAAP I believe measures at 670 nm where brown carbon should absorb very little. Also the sentence "Secondly, MAAP detects practically all absorbing particles" can be deceiving as one might interpret it as if the MAAP could detect also all BrC and all dust, which would not be true if not absorbing at 670 nm. Maybe the authors mean "all rBC" instead of "all absorbing particles"?

Reply:

Brown carbon is not mentioned anymore. The second sentence was referring to the detection range (limited size range for SP2, but not for MAAP), which is now clarified.

Changes to the manuscript:

Line 421: "First of all, ~~rBC is a fraction of eBC, which can contain non-refractory~~ eBC detected by MAAP can contain light absorbing organics ~~such~~ generally referred as brown carbon~~. Secondly, MAAP detects practically all absorbing particles, but~~ (e.g. Bond et al., 2013). Since brown carbon is typically non-refractory and weakly absorbing at the near-infrared wavelengths, it cannot be detected by the SP2. … Secondly, SP2 sizing is limited to 75–655 nm rBC core volume equivalent diameter range. Although larger rBC particles, which ~~saturate the incandescence detectors~~can be detected but not sized, were rarely observed,"

- Lines 371-376: This paragraph is a little bit hard to read and understand. Either I do not understand clearly the different models, or the internally mixed homogeneous model seems very unrealistic. A cartoon of the different mixing scenario might help much more than the written explanation.

Reply: A cartoon has been added.

Changes to the manuscript: Several - please see the updated Sect. 3.5 and Fig. 7.

- Line 382: the placement of the right ")" seems incorrect.

Reply: This was intentional, but we have now removed the parenthesis.

Changes to the manuscript:

Line 532: "…fraction is ~~(~~0.24/2.0^3 =~~)~~ 0.03…"

- Line 406: the surface albedo used is fairly low here. Please justify the choice; for example, considering that at the site the albedo might be much higher if snow is present.

Reply: The used surface albedo is typical for forests seasonally coved by snow. It is a fact that the absolute values of the surface albedo and most other parameters in this equation are not well known. Since our purpose is not to give exact RFE values, but to compare different mixing state models, slight inaccuracies can be tolerated. The equation itself is also a great simplification of a difficult radiative transfer problem, but good for our purpose. We have now clarified this.

Changes to the manuscript:

Line 570: "Although Eq. (1) is highly simplified solution for a complex problem and its parameters have uncertainties, which means that the absolute RFE values are not fully accurate, this equation is suitable for comparing different mixing state models."

Caption of figure 5: I would change "correlation" to "slope" or "line" in "The dashed line shows 1:1 correlation."

Reply: Done.

Changes to the manuscript:

Figure 6 caption: "The dashed line shows 1:1 ~~correlation~~slope."

Anonymous Referee #2

This study provides valuable data in the Arctic ground site, however needs to address the followings:

Major: The introduction part I would suggest to shorten the part which explains the BC instrumentation, but more focusing the BC measurements in the Arctic ground sites.

Reply:

We have now given more details about the surface BC in the Arctic with the focus in study area. We have also slightly shortened the part explaining BC instrumentation.

Changes to the manuscript: Several - please see the marked up manuscript (Sect. 1)

About SP2- 1. Has the Aquadag calibration been applied to the ambient, i.e. different instrument response to Aquadag and ambient BC. 2. I would suggest to use an inverted Mie table to calculate the Dp/Dc using core refractive index 2.26+1.26i and coating 1.5+0i [Taylor et al., 2015; Liu et al., 2014]. 3. It is better to show a Dp and Dc size distribution for BC, and Dp size distribution for scattering particle to explicitly explain how you calculate the rBC number fraction.

Reply:

1. No, because we do not have tools to determine the difference in instrument response between Aquadag and ambient Arctic rBC. To our knowledge, there are no previous studies from the Arctic where the difference has been reported. This potential bias is mentioned when SP2 and MAAP results are being compared.

2. We have previously used this method, but considering the uncertainties related to particle morphology, LEO method, detections limits and optical constants, it is difficult to say if this improved the results or not. At this point we are assuming that all particles scatter light as pure ammonium sulfate. This is also consistent with our updated terminology where core-shell model is not presumed (see the comment by Referee #1 and our response). Since this is still an open question in the SP2 community, we aim to take a neutral position.

3. We have now simplified this section especially regarding the LEO method. Adding more technical details (the suggested figure) would make this section less clear. The calculations are actually very simple: we just

calculate number concentrations by integrating the relevant size distributions over the same particle (LEO) size range.

Changes to the manuscript: Several - please see the marked up manuscript (Sect. 2.2)

About the result analysis 1. To me, the Dp/Dc ranges 1.7-2.2, GMD 150nm-240nm; BC number fraction 0-0.5. All of these variations are significant. There must be very interesting stories there however have not been fully analysed and explained. 2. A general look of Fig. 3 is the BC mass is significantly lower in cloud than no cloud, does that mean a fraction of BC has been scavenged? Have you removed the data when snow precipitation? 3. About section 3.2.1, again when you have fully explained your own story, the comparison will be more interesting however at the moment the base is not solid. 4. There is no much point for section 3.2.2, as there will be no apparent diurnal trend for this remote site. 5. Could we show the clustered air mass types in Fig.3. 6. For section 3.4, I would suggest to calculate the MAC (absorption/mass) for different air masses, is rBC size or coating thickness affecting MAC?

Reply:
1. Yes, these variations are significant, but not as large as those of the rBC mass concentration. It seems that the lack of correlation between these variations (except that of rBC mass concentration) and those of the other parameters is the most interesting story. The lack of correlation (or the correlation for total rBC mass) is now explained in the results section.

Changes to the manuscript: Several - please see the marked up manuscript (especially Sects 3.2 and 3.3)

Reply:
2. As mentioned in the text, significant correlation was not found between BC mass and clouds. This is good for us, because clouds could have caused a bias to our results, but the lack of correlation shows that other factors than clouds (mainly activation and removal by the PM10 inlet) dominate (in-cloud scavenging, precipitation, etc. may have altered the size distributions any time before the observation at Pallas, but we do not have tools to examine that). Snow fall events were not removed from the data. These could not be examined in detail, because, the weather station had low data coverage. On the other hand, the observed snow fall events occurred during in-cloud events (no precipitation during most of the in-cloud events), which are examined.

Changes to the manuscript:
Sections 2.2 and 3.2.1: Several updates related to the presence of clouds and precipitation - please see the marked up manuscript
Line 314: "There are some cases where the changes in the observed aerosol parameters (mainly rBC mass concentration) can be related to the appearance or disappearance of clouds, but most of the observed variability is caused by other factors such as air mass history. Statistical analysis (not shown) ~~was also performed to confirm~~ also confirmed that the average aerosol properties were similar during no cloud and in cloud time periods."

Reply:
3. In this section we have compared our numerical mean values with those from other campaigns. More qualitative comparison of "stories" with that from a similar study would be interesting, but currently this is the first appearance of long-term SP2 ground study from Arctic.

Changes to the manuscript: Several - please see the marked up manuscript (Sect. 2.2)

Reply:

4. The absence of diurnal variations of the mixing state parameters is a result itself. We have also observed a diurnal cycle for rBC concentration when polar night and early spring are considered separately. Therefore, keeping this short section is justified.

Reply:

5. We have added trajectory directions (and CO concentration) to Fig. 3 so that the marker color is based on the trajectory direction.

Changes to the manuscript: Please see updated Fig. 3

Reply:

6. We did some additional calculations where we tried to correlate rBC to eBC ratios (can be related to MAC) with trajectory directions and rBC mixing state parameters (mean size, rBC number fraction and particle to core diameter ratio), but significant correlations were not found. Therefore, these are not shown in the paper.

Changes to the manuscript: Several - please see the marked up manuscript (Sect. 3.4)

Specific: Abstract "On the average, the number fraction of particles containing rBC was 0.24 and the average rBC core size in these particles was half of the total size (coated to core diameter ratio was 2.0). These numbers mean that the core was larger and had a significantly thicker coating than in typical particles closer to their source regions."

State the number fraction of rBC is for what size range of particles –PM1? These numbers means core 'larger'? It is not surprising the BC in this remote site is thickly coated, so does not mean too much if compared to 'sources'. 'Comparison of the measured rBC mass concentration with that of the optically detected equivalent black carbon (eBC) showed a factor of five difference, which could not be fully explained without assuming that a part of the absorbing material is non-refractory.' – part of the absorbing material is non-refractory, what does that mean.

Reply:

Size ranges for the calculations are now given. We have now clarified that rBC core size is typical for aged air masses, but particle to rBC core volume equivalent diameter ratio is higher than in most other studies. We have also clarified that only a part of the light absorbing material is refractory and absorbs light at the wavelength used by the SP2.

Changes to the manuscript:

Line 8: "The rBC mass was log-normally ~~distributed rBC core size was relatively constant with an average geometric~~ distributed showing a relatively constant rBC core mass mean diameter with an average of 194 nm(75–655 nmsizing range). On the average, the number fraction of particles containing rBC was 0.24 (integrated over 350–450 nm particle diameter range) and the average ~~rBC core size in these particles was half of the total size (coated to core~~ particle diameter to rBC core volume equivalent diameter ratio was 2.0 (averaged over particles with 150–200 nm rBC core volume equivalent diameters). These average numbers mean that the ~~core was larger and had a significantly thicker coating than in typical particles closer to their source regions~~ observed rBC core mass mean diameter is similar to those of aged particles, but the observed particles seem to have unusually high particle to rBC core diameter ratios. Comparison of the measured rBC mass concentration with that of the optically detected equivalent black carbon (eBC) ~~showed~~ using an Aethalometer and a MAAP showed that eBC was larger by a factor of five ~~difference, which~~ . The difference could not be fully explained without assuming that only a part of the optically detected light absorbing material is ~~non-refractory~~ refractory and absorbs light at the wavelength used by the SP2."

Manuscript prepared for Atmos. Chem. Phys.
with version 2014/09/16 7.15 Copernicus papers of the LaTeX class copernicus.cls.
Date: 24 August 2015

Black carbon concentrations and mixing state in the Finnish Arctic

T. Raatikainen, D. Brus, A.-P. Hyvärinen, J. Svensson, E. Asmi, and H. Lihavainen
Finnish Meteorological Institute, Helsinki, Finland
Correspondence to: T. Raatikainen (tomi.raatikainen@fmi.fi)

Abstract. Atmospheric aerosol composition was measured using a Single Particle Soot Photometer (SP2) in the Finnish Arctic during winter 2011–2012. The Sammaltunturi measurement site at the Pallas GAW (Global Atmosphere Watch) station receives air masses from different source regions including the Arctic Ocean and continental Europe. The SP2 ~~is a unique instrument that can give~~ provides detailed information about mass distributions and mixing state of refractory black carbon (rBC). ~~As expected, the~~ The measurements showed widely varying rBC mass concentrations (0–120 $\mathrm{ng\,m^{-3}}$), which were related to varying contributions of different source regions and aerosol removal processes. The rBC mass was log-normally ~~distributed rBC core size was relatively constant with an average geometric~~ distributed showing a relatively constant rBC core mass mean diameter with an average of 194 nm (75–655 nm sizing range). On the average, the number fraction of particles containing rBC was 0.24 (integrated over 350–450 nm particle diameter range) and the average ~~rBC core size in these particles was half of the total size (coated to core~~ particle diameter to rBC core volume equivalent diameter ratio was 2.0 (averaged over particles with 150–200 nm rBC core volume equivalent diameters). These average numbers mean that the ~~core was larger and had a significantly thicker coating than in typical particlescloser to their source regions~~observed rBC core mass mean diameter is similar to those of aged particles, but the observed particles seem to have unusually high particle to rBC core diameter ratios. Comparison of the measured rBC mass concentration with that of the optically detected equivalent black carbon (eBC) ~~showed~~ using an Aethalometer and a MAAP showed that eBC was larger by a factor of five~~difference, which~~ . The difference could not be fully explained without assuming that only a part of the optically detected light absorbing material is ~~non-refractory~~refractory and absorbs light at the wavelength used by the SP2. Finally, climate implications of five different ~~rBC~~ black carbon mixing state representations were ~~quantified~~ compared using the Mie approximation and simple direct radiative forcing efficiency calculations. These cal-

culations showed that the observed mixing state ~~(separate non-absorbing and coated rBC particles)~~ means significantly lower warming effect or even a net cooling effect when compared with that of an homogenous aerosol containing the same amounts of ~~rBC~~ black carbon and non-absorbing material.

1 Introduction

~~Most atmospheric~~ Atmospheric aerosols scatter incoming solar radiation and therefore have a cooling effect on climate, but ~~especially black carbon aerosols~~ certain aerosol species such as black carbon also absorb solar radiation, which means that they can have a warming effect (IPCC, 2013; Bond et al., 2013). ~~Absorbing~~ Light absorbing aerosols have the largest warming effect over reflective surfaces such as clouds, snow and ice. In addition, deposition of absorbing aerosols on snow and ice decreases surface reflectivity which further enhances snow melt ~~and decreases surface reflectivity~~ (e.g., Hansen and Nazarenko, 2004; Flanner et al., 2007; Svensson et al., 2015). Most of the submicron aerosol light absorption is caused by the broadly defined black carbon ~~(BC)~~(Petzold et al., 2013), but there are also organic ~~compounds~~ carbon particles that absorb especially at ultraviolet wavelengths (so-called brown carbon) and dust which is the main absorbing aerosol type for super micron particles (Bond et al., 2013). Atmospheric general circulation models are used to quantify climate effects of ~~BC~~ black carbon (BC) aerosols, but it is known that these models are not ~~always~~ accurate in simulating the complex aerosol lifecycles including formation, aging, transportation, cloud interactions, and removal processes (e.g., Kipling et al., 2013; Stohl et al., 2013; Genberg et al., 2013; Dutkiewicz et al., 2014; Wang et al., 2014a). This means that the model predicted aerosol concentrations and mixing state are ~~not always~~ generally not in agreement with the observations. Detailed aerosol composition and mixing state measurements are therefore needed to assess model accuracies and to improve model ~~parameters~~ parameterizations (Reddington et al., 2013; Schwarz et al., 2013; Samset et al., 2014; Wang et al., 2014b).

Aerosol interactions with radiation and water vapor depend on the mixing state of the absorbing material ~~(e.g., Cappa et al., 2012)~~(e.g., Adachi et al., 2010; Cappa et al., 2012). For example, ~~it~~ the absorbing material can be distributed so that a large fraction of particles contain small amounts of absorbing material or vice versa. ~~By definition~~From the optical point of view, an aerosol population is externally mixed when not all particles are absorbing and internally mixed when all particles are absorbing. Individual ~~particles can also have different structures such~~ absorbing particles have wide range of structures starting from small spherules which form chain-like aggregates and usually end up being densely packed clusters mixed with non-absorbing material (e.g. Bond et al., 2013). Typical radiative transfer models describe these as bare or coated black carbon ~~particle~~ particles or a homogenous mixture of black carbon and non-absorbing compounds. For the unit mass of an absorbing material, internally mixed coated particles absorb more than externally mixed bare particles due to the increased effective cross sectional area (e.g., Schwarz et al., 2008b). In addition,

aerosol interactions with water vapor, which are important for optical properties of droplets and clouds as well as for wet removal processes, depend on the mixing state (e.g., Zhang et al., 2008; Liu et al., 2013). For example, the capability of the initially hydrophobic black carbon particle to act as a cloud condensation nuclei (CCN) increases ~~with increasing coating thickness~~when coated or mixed with material that is hygroscopic.

There are several instruments for measuring ~~total black carbon~~ black carbon mass concentrations, but few instruments are able to give any information about the mixing state. The Single Particle Soot Photometer or briefly SP2 (Stephens et al., 2003; Schwarz et al., 2006; Moteki et al., 2007) is probably the most versatile and widely used instrument for measuring mass distributions and mixing state of refractory black carbon (rBC). Refractory black carbon is the fraction of the absorbing carbonaceous material that has boiling point close to 4000 K and emits visible light when heated to that temperature (Petzold et al., 2013; Lack et al., 2014). ~~This means that non-refractory absorbing material such as brown carbon cannot be detected by the SP2.~~

Long term ~~black carbon measurements by~~ measurements of elemental carbon by optical and thermal-optical methods show that concentrations have been decreasing in the Finnish Arctic during the last four decades due to the decreased emissions (Dutkiewicz et al., 2014). On the annual scale, the highest ~~BC~~ concentrations are seen during winter and early spring (Hyvärinen et al., 2011; Dutkiewicz et al., 2014). ~~Modelling~~ At that time air masses are typically stable with low boundary layer heights, which allows the accumulation of aerosol pollutions. Also, winter is the season when domestic heating by burning wood produces largest black carbon emissions. A modelling study by Stohl et al. (2013) showed that the majority of the observed black carbon is from domestic combustion, but industrial sources and long-range transport have also a significant effect. Although there are a few previous airborne SP2 measurements covering the Arctic ~~(e.g., Samset et al., 2014)~~(e.g., Baumgardner et al., 2004; Samset et al., 2014), they provide a snapshot of rBC mixing state at a specific altitude and location. Long term surface measurements are also needed as they provide boundary conditions for the vertical distributions and also show how concentrations vary as a function of time (diurnal and annual cycles, aerosol sources and removal processes).

The main purpose of this study is to provide new experimental information about the rBC mass distributions and mixing state ~~at~~ in the Finnish Arctic. The SP2 measurements were conducted at Pallas GAW (Global Atmosphere Watch) station from December 2011 to February 2012. To our knowledge, these are the first published ~~long-term~~ medium term surface SP2 results from the area and also from the Fennoscandian Arctic. In addition to the mixing state information, trajectory analysis is used to estimate the sources of rBC and the effects of different sources on rBC mixing state. We ~~will~~ also compare rBC concentrations with those derived from filter-based optical measurements to see if these are in agreement or depend on the physical properties (e.g. volatility) of black carbon. Finally, climate implications of different black carbon mixing state representations constrained by

our observations are assessed based on a Mie approximation and a simple direct radiative forcing efficiency model.

2 Experimental

2.1 Pallas measurement station

Figure 1 shows the location of the Pallas Global Atmosphere Watch (GAW) station at the northern edge of continental Europe. Measurements were conducted on a top of a fell called Sammaltunturi (67°58.400′ N 24°6.939′ E, 565 m a.m.s.l.) about 250 m above surrounding sparsely populated hilly terrain covered by mixed pine, spruce and birch forests (Hatakka et al., 2003). In the absence of significant local aerosol sources, most observed particles are long-range transported from the Kola Peninsula and from more densely populated and industrialized areas from the south. Therefore, Pallas is a site where relatively well aged air masses can be observed on their way to the north. On the other hand, the site also receives clean air masses from the north.

2.2 Instrumentation

The station has ~~stationary instruments for measuring~~ instruments for continuous measurements of meteorological parameters, trace gases and aerosol size distributions and optical properties (Hatakka et al., 2003). During the Pallas winter campaign, a Single Particle Soot Photometer (SP2; Revision C* with 8 channels) manufactured by Droplet Measurement Technologies (Boulder, CO, USA) was used to measure size distributions and mixing state of refractory black carbon (rBC). ~~Brief~~ We focus on the SP2 measurements, but a brief description of the ~~instrument, data processing and calculated parameters are given in Sect. "Single Particle Soot Photometer (SP2)".~~ optical black carbon and trace gas measurements is given below.

The measurement station has three sample lines: one is without nominal cut-off diameter (the total line)~~and the other lines have about 5~~, one has a cyclone for removing particles larger than 10 µm (~~the gas~~ PM_{10} line) and the third one is so-called gas line where inlet design limits the particle size to about 5 µm. The station is located on top of a fell, which means that it is often covered by low level clouds. Cloud droplets are formed when water condenses to existing aerosol particles. Since cloud droplets are often larger than 10 µm~~(~~, those particles that have formed cloud droplets are missing from the gas and PM_{10} ~~line) cut-off sizes. The~~ sample lines. Because the SP2 was connected to the PM_{10} sample line, ~~which means that some ice nuclei (IN) and cloud condensation nuclei (CCN) are not detectable when the station is covered by clouds. These~~ results can be biased during these in cloud events. Similarly, precipitation can decrease aerosol concentrations by washing out particles. Such in cloud and precipitation events can be identified and possibly filtered using visibility and precipitation data, respectively, from the weather station. Unfortunately, the weather station had only 32 % data coverage for the campaign period. Alternative methods can be used to identify the in

cloud events, which also include most of the precipitation events as precipitation is strongly related to the presence of low level clouds.

Since the weather station data is largely missing, in cloud time periods are found by comparing particle number size distributions from two Differential Mobility Particle Sizers (DMPS; see Hatakka et al. (2003) or Komppula et al. (2005) for the description of the measurement setup and instruments). One DMPS was connected to the total line (all particles) and the other was connected to the gas line (~~IN and CCN removed at the inlet~~no particles from cloud droplets). The difference between the total and gas sample line size distribution gives the dry size distribution of ~~IN and CCN~~particles from cloud droplets, which are typically larger than 100 nm in dry diameter (Komppula et al., 2005). In our analysis, the relative difference (i.e. activated fraction) for 260–465 nm dry size range which is larger than 0.8 is considered as an in cloud case and a value smaller than 0.2 indicates clear conditions at the station; the remaining points indicate missing DMPS data or unclear or variable cloud conditions. It should be noted that this definition is designed for our purpose since it shows when clouds have a large effect on the observations (more than 80 % of the large particles missing) and when there are no clouds or clouds have a negligible effect on the observations (less than 20 % of the large particles missing).

The station has two continuously operating instruments for absorption measurements (for details see e.g. Hyvärinen et al., 2011; Lihavainen et al., 2015). Thermo Scientific ® 5012 Multiangle Absorption Photometer (MAAP) and ~~seven-wavelength~~ Magee Scientific Corporation AE31 7-wavelength Aethalometer collect aerosols to a filter and measure the change in light attenuation. This is then converted to equivalent black carbon (eBC) mass concentration by using instrument specific parameters (e.g. Petzold and Schönlinner, 2004; Hansen et al., 1984). MAAP data was used as is, but Weingartner correction (Weingartner et al., 2003) was applied to the Aethalometer data. ~~The MAAP~~ Through discussion of the instrument uncertainties can be found elsewhere (e.g. Lack et al., 2014), but the reported uncertainty for MAAP is about 12 % and it is considered to be more accurate than the Aethalometer. Here we are focused on the MAAP data, because it was connected to the same PM_{10} sample line as the SP2 ~~, which means that their reported eBC and rBC concentrations are always comparable, but both can be biased during the in cloud conditions. The~~ while the Aethalometer was connected to the total sample line.

Since some trace gases are co-emitted with the aerosol black carbon, comparison of rBC and gas concentrations can give an indication of rBC sources and the age of the air masses. Concentrations of carbon monoxide and dioxide (CO and CO_2), nitrogen dioxide (NO_2), sulfur dioxide (SO_2) and ozone (O_3) were measured using instruments described by Hatakka et al. (2003), except that CO and CO_2 are more recently measured by a Picarro, Inc., CRDS (Cavity Ring-Down Spectroscopy) analyzer ~~. Since some of these gases are co-emitted with the aerosol black carbon, comparison of rBC and gas concentrations can give an indication of rBC sources and the age of the air masses.~~ (model G2401).

~~Single Particle Soot Photometer (SP2)~~

Detailed description of the ~~instrument~~ SP2 operation principles is given elsewhere (e.g., Stephens et al., 2003; Schwarz et al., 2006; Moteki et al., 2007). Briefly, sample aerosol particles travel through a ~~powerful laser beam, where non-absorbing and absorbing particles are identified based on the scattered laser light and emissions of~~ laser cavity (1064 nm wavelength), where absorbing refractory particles are quickly heated to a temperature where they emit visible light (laser-induced incandescence)~~, respectively~~. The maximum incandescence signal is proportional to the refractory black carbon (rBC) mass and this dependency is parameterized using size-selected Aquadag® (Acheson Inc., USA) particles, ~~which~~ whose masses are calculated using the density parameterization from Gysel et al. (2011). This calibration gives ambient rBC particle mass (0.4–260 fg ~~) as a function of measured incandescence signal amplitude; rBC core~~ mass quantification range) and rBC volume equivalent diameter (75–655 nm sizing range) is then calculated from the mass by assuming $1800\,\mathrm{kg\,m^{-3}}$ ~~particle density . Non-absorbing~~ rBC density and spherical void-free particles. It should be noted that the real particle structure is typically more complex than just a compact rBC core coated by a non-refractory material (e.g. Bond et al., 2013). All particles scatter laser light so that the maximum scattering signal is proportional to the scattering cross section of the particle, which ~~is calculated~~ can be related to particle size and optical constants using the Mie approximation (e.g., Bohren and Huffman, 1983). If a particle contains absorbing material, its maximum scattering signal is decreased due to the evaporation of the non-refractory material. However, the unperturbed maximum scattering signal can be reconstructed using so-called Leading Edge Only (LEO) method (Gao et al., 2007; Metcalf et al., 2012). Again, calibration experiments ~~are used to relate calculated scattering cross sections of~~ with size-selected ammonium sulfate particles ~~to the observed scattering signal amplitudes. This calibration gives scattering cross sections for ambient particles, so their exact sizes depend on particle shape, structure and refractive index. In practice,~~ are used to relate observed (or reconstructed) scattering signals to actual particle sizes. For this calibration we have assumed that ambient particles are spherical and optically similar to ammonium sulfate~~even when they contain rBC. This means that the scattering particle~~ . The sizing range is 190–535 nm ~~.~~

~~Additional analysis is required to calculate sizes of coated rBC particles. The scattering signal is first Gaussian following the Gaussian laser beam profile, but reduces from that when the coating starts to evaporate. The unperturbed scattering signal amplitude can be reconstructed using so-called Leading Edge Only (LEO) method (Gao et al., 2007; Metcalf et al., 2012). In practice, a Gaussian scattering signal profile with known peak position and width is fitted to~~ for non-absorbing particles. Because evaporation of non-refractory material decreases signal to noise ratio, the ~~Gaussian section of the observed scattering signal (the leading edge) by adjusting peak height. Peak positions and widths are obtained from those of purely scattering particles: the width is simply the width of the observed scattering signal and peak position is based on the observed lag time from a Two-Element Avalanche Photodiode (TEAPD) detector signal to the scattering peak position. In the current~~

~~calculations, the widths and the lag times are calculated as a standard deviation weighted running mean using values from 100 previous purely scattering particles. The leading edge fit includes points where the Gaussian signal is between 1/1500 and 1/30 of the maximum value. LEO fits can be made when the leading edge scattering signal exceeds noise and the TEAPD signal is valid; for the current SP2 this means that coated particle size must be at least~~ lower sizing limit for absorbing particles is about 300 ~~nm~~ nm.

SP2 intercomparison experiments by Laborde et al. (2012b) have shown that the measurement uncertainty for calibration experiments using different SP2 instruments range from 5 % to 17 % being the smallest for rBC number and the largest for the size of coated rBC particles. These uncertainties can be considered as a lower limit for the current field measurements. In addition to the typical uncertainties, the results can be biased due to the possible differences between calibration and ambient particle properties such as sensitivity (signal response to a known rBC mass), density, morphology and refractive index (e.g. Moteki and Kondo, 2010; Laborde et al., 2012b, a; Baumgardner et al., 2012; Lack et al., 2014; Taylor et al., 2015). Since these properties are not determined for Arctic aerosol, there is a possibility for a bias that can be larger than the typical measurement uncertainty. More discussion about the potential bias is given in Sect. 3.4.

Hourly average mass and number size distributions ~~(40 logarithmic size bins)~~ and mixing state parameters (number fraction of particles containing rBC and ~~coated to core~~ particle diameter to rBC core volume equivalent diameter ratios for those particles) are calculated from the single particle data. Concentrations are ~~calculated using recorded sample flow rates at~~ given at the instrument temperature and pressure. The number fraction of rBC containing particles ($N_{\mathrm{rBC}}/N_{\mathrm{total}}$) is calculated from the ~~rBC and non-absorbing particle~~ number size distributions ~~measured by the SP2. The number concentration of rBC containing particles (N_{rBC}) is calculated by integrating the rBC number size distribution over~~ using 350–450 nm ~~LEO (or coated particle) size range. Similarly, the number concentration of non-absorbing particles (the total is the sum of rBC containing and non-absorbing particles) is calculated from the non-absorbing particle number size distribution using the same LEO size range (LEO size used for consistency)~~ particle size (calculated using the LEO method) range. The 350–450 nm ~~integration LEO~~ size range is selected considering LEO sizing limits ~~and counting statistics. The lowest particle size ((~~reliable results for particles larger than 350 ~~nm) is large enough so that reliable LEO fits can be made and the size range from 350 to 450 nm contains enough particles for~~ nm) and reasonable counting statistics (enough particles in this size range). In practice, this size range is representative of the typical ~~coated accumulation mode rBC~~ accumulation mode particles. The first results showed that practically all rBC particles ~~are coated by a~~ contain non-refractory material~~(core-shell structure assumed). Because absolute coating thickness depends on particle size so that larger particles have typically thicker coatings, a relative parameter is better for averaging. Here relative coating thickness is defined as coated (from~~ . The relative amounts of rBC and non-

refractory material in a particle is described by an average particle diameter (from the LEO method) to ~~core diameter ratio~~rBC core volume equivalent diameter ratio (briefly particle to rBC core diameter ratio), D_p/D_{rBC}~~, and it is calculated as~~ . The parameter is an average of those of individual rBC containing particles which rBC core ~~diameter (D_{rBC})~~ volume equivalent diameter is 150–200 nm. This 150–200 nm rBC core size range has enough particles for good counting statistics and it is in the range where ~~typical coating thicknesses are accounted for~~particle sizes can be calculated using the LEO method.

The initial SP2 data analysis showed that some results were dependent on the SP2 chamber temperature, which ranged from 23 to 33 °C during the campaign. ~~By comparing measured rBC concentration with the equivalent BC (eBC) measured by MAAP, it was concluded that the~~ Instrument inter-comparison showed that the SP2 ~~undercounted rBC~~ underestimated rBC compared to the eBC derived from the MAAP, when SP2 temperature decreased below 25 °C, so this SP2 data was ignored. Careful inspection of the SP2 data showed that laser power was most likely decreased below the minimum required for heating rBC particles to their boiling point. Namely, decreasing temperature and laser power meant that particles reached their boiling points closer to the center of the laser beam. This means that particles that miss the center of the laser beam (particle beam width is about 25 % of the laser beam width; Laborde et al., 2012b) do not always reach their incandescence temperature and therefore are not detected as rBC. When laser power is high enough, incandescence signal is practically independent of the laser power, but scattering signal is always proportional to the laser power. However, comparison of scattering particle size distributions and particle size distributions from DMPS showed that the instrument temperature could have caused about 10 % bias to the scattering size, which is smaller than the typical sizing uncertainty of the instrument. The weak temperature dependency is partly explained by the fact that the scattering detector gain is also temperature dependent, but so that the gain (signal) increases when laser power decreases (SP2 workshop communications, Boulder, CO, USA, 2014). In addition, scattering size ~~is~~ calculated from the calibration is roughly proportional to the logarithm of the ~~signal,~~ maximum scattering signal, which is proportional to the laser power, so even a 50 % change in laser power would have a minor effect on the calculated scattering size.

2.3 Trajectories

Five ~~days long~~ day backward trajectories were calculated using the HYSPLIT model (Draxler and Hess, 1997, 1998; Draxler, 1999). Trajectory end point altitude was set to 500 m a.g.l. Trajectory calculations were initiated every three hours and coordinate points were saved hourly (120 coordinate points in addition to the end point). ~~Each trajectory is represented by two parameters: average distance and direction. These~~ Parameters describing average altitude above ground level, total length, average direction and average distance were calculated for each trajectory. Average distance and direction are the magnitude and direction of a vector calculated as an average of vectors pointing from

Pallas to each of the hourly trajectory coordinate points. The vectors from Pallas to the trajectory coordinate points were initially converted from spherical (latitude and longitude degrees) to Cartesian coordinates (kilometers). Average distance and direction indicate the distance and direction of the source area from the Pallas measurement station, respectively. Trajectories originating from Central Europe and southern Finland have similar average directions, but these can be distinguished based on the average distance.

3 Results

3.1 Meteorology

Ambient temperature was initially about $-2\,^{\circ}\mathrm{C}$ (hourly averages), but decreased throughout the campaign reaching $-24\,^{\circ}\mathrm{C}$ at the end. Snowfall was observed occasionally, but these and visibility observations were missing from most days (32 % data coverage). ~~Campaign~~ The campaign average wind speed was $9\,\mathrm{m\,s^{-1}}$ and the hourly averages were between 1 and $17\,\mathrm{m\,s^{-1}}$. The S–SW was the most frequent wind direction sector and the second was NE–E. ~~Trajectory analysis gave~~ The trajectory analysis gave a slightly different view of the origin of the air masses with the dominating sector centered at SE (Eastern Europe) and a minor sector at E (Kola Peninsula). The campaign started 17 December 2011 during the polar night, which lasts about 3.5 weeks at that location, but at the end of the campaign (2 February 2012) the daily maximum solar radiation reached $30\,\mathrm{W\,m^{-2}}$.

3.2 rBC properties

Figure 2 shows campaign averages of rBC mass and number size distributions ~~. The~~ (shown as a function of rBC core volume equivalent diameter). The peak of the number size distribution ~~extends well below~~ seem to be unresolvable due to the 75 nm detection limit, which means that distribution parameters (total number, mode and width) cannot be calculated or determined from a fit to the data. On the other hand, the observed rBC mass seem to be centered within the sizing range (75–655 nm). For example, using the log-normal fit to extrapolate rBC mass concentration would give $27\,\mathrm{ng\,m^{-3}}$ when the integrated rBC mass is $26\,\mathrm{ng\,m^{-3}}$. ~~Therefore, calculated~~ Because extrapolation is not needed, log-normal mass distribution parameters (total mass concentration, geometric mass mean diameter and geometric standard deviation) ~~will be~~ calculated from the observations are used to describe rBC mass ~~distribution~~distributions. Because geometric standard deviation is fairly constant, we ~~will~~ focus on the total mass concentration and geometric mass mean diameter.

Figure 3 shows the time series of the main rBC properties including the total mass concentration (c_{rBC}) ~~,~~and geometric mass mean diameter ($\mathrm{GMD_{rBC}}$) for the 75–655 nm rBC core diameter detection range, number fraction of particles containing rBC ($N_{\mathrm{rBC}}/N_{\mathrm{total}}$; calculated using 350–450 nm particle size range), and ~~coated to~~ particle to rBC core diameter ratio ($D_{\mathrm{p}}/D_{\mathrm{rBC}}$; calculated using 150–200 nm rBC core size range). Background color indicates when the station is in cloud (blue)

and when not (red), and when the presence of clouds is unclear or the DMPS data is missing (white). As explained in Sect. 2.2, SP2 measurements can be biased during the in cloud time periods, because ~~some ice and cloud condensation nuclei become too large to be detected~~most activated particles are removed by the inlet system. There are some cases where the changes in the observed aerosol parameters (mainly rBC mass concentration) can be related to the appearance or disappearance of clouds, but most of the observed variability is caused by other factors such as air mass history. Statistical analysis (not shown) ~~was also performed to confirm~~ also confirmed that the average aerosol properties were similar during no cloud and in cloud time periods. Therefore, we ~~will~~ use the full data set in the following calculations.

Average rBC mass concentration (the data shown in Fig. 3) is 26 $\mathrm{ng\,m^{-3}}$, but the values range from about zero to 120 $\mathrm{ng\,m^{-3}}$ (Fig. 3). Average geometric mass mean diameter is 194 nm and 90 % of the values are between 161 and 231 nm. The average number fraction of particles containing rBC is 0.24 and again 90 % of the values are between 0.14 and 0.35. Finally, the average ~~coated to~~ particle to rBC core diameter ratio is 2.0 and the 90 % limits are from 1.8 to 2.1. ~~Although especially~~ Figure 3 and the 90 % limits show that the rBC mass concentration varies significantly ~~, rBC number fraction and coated to core diameterratio have relatively constant values~~more than the mixing state parameters and the geometric mass mean diameter.

3.2.1 Comparison with other SP2 studies

One complication in comparing SP2 results from different groups and locations is that different calibration materials are being used (e.g. Aquadag® or fullerene soot; Moteki and Kondo, 2010; Laborde et al., 2012a; Baumgardner et al., 2012) and different optical and physical properties (e.g. refractive index, particle structure and density) are assumed for the ambient rBC and scattering material. There are also different ways to calculate mixing state parameters (e.g. size range). To our knowledge, this is the first published SP2 study where ~~long-term~~ medium term surface measurements have been conducted at high latitudes during Arctic winter, so direct comparison with other studies is not possible. Nevertheless, published studies can give an idea of how Pallas rBC properties are related to those from different environments.

~~In general, rBC observed at Pallas is long-range transported and aged. As a result, rBC mass concentrations are lower and particles are larger than in air masses observed closer to their source regions (e.g., Huang et al., 2012; Reddington et al., 2013; McMeeking et al., 2010). Although rBC mass concentrations and mean diameters are commonly reported, there is less information about the~~ The observed rBC mass concentration and mean diameter are generally similar to those observed at higher altitudes or from aged air masses (e.g., Huang et al., 2012; Reddington et al., 2013; McMeeking et al., 2010). As these parameters are relatively well known, we focus on the less studied rBC mixing state (~~rBC coating thickness and~~ number fraction of rBC containing particles and particle to rBC core volume equivalent diame-

ter ratio for these particles). Previous airborne measurements have shown that the ~~relative coating thickness~~ diameter ratio (D_p/D_{rBC}) is typically close to 1.5 in long-range transported urban and biomass burning plumes (e.g., Kondo et al., 2011; Schwarz et al., 2008a; Sahu et al., 2012; Metcalf et al., 2012), which is significantly smaller than the 2.0 observed at Pallas. Even larger diameter ratios (2.4 for 170 nm rBC core size) have been observed in an aged (3–4 days) smoke plume, but this is partly caused by the low rBC core size with mass median diameters ranging from 120 to 160 nm (Dahlkötter et al., 2014). There is very little published information about the number fraction of particles containing rBC especially ~~at~~ in the aged air masses. The closest match with our study is the study of Reddington et al. (2013) who used rBC measurements and model information to estimate that 14 % of particles larger than 260 nm contain rBC in the European lower troposphere (altitude less than 2.5 km above ground level). This fraction is again significantly smaller than the 24 % observed at Pallas. ~~One possible explanation is that cloud processing increases rBC coating thickness (condensation~~ Cloud processing during the long transport from source areas to Pallas is a possible explanation for the high values of particle to rBC core diameter ratio and rBC number fraction. Condensation of semi-volatile species ~~and coagulation) and removes more hygroscopic particles (wet deposition) during the transport from source areas to Pallas~~to cloud droplets and in-cloud scavenging increase the particle to rBC core diameter ratio. It is also possible that the rBC number fraction increases, because wet deposition favors the more hygroscopic rBC-free particles.

In addition to the basic mixing state parameters, careful examination of the scattering and incandescence signals can ~~show if the rBC particles are coated or not and if the particles have core-shell~~ give an additional information about the particle structure. For example, Huang et al. (2012) summarizes number fractions of ~~coated~~ particles containing both rBC and non-refractory material (called internally mixed in their paper~~) rBC~~ , but here this term is reserved for particle populations) from several studies (environments) and shows that the number fraction varies between 3 and 80 % (the rest of the rBC containing particles are pure rBC). Although different calculation methods can lead to lower values~~(thin coatings cannot be detected from small rBC particles)~~, these numbers are much smaller than that observed at Pallas where practically 100 % of rBC ~~particles are coated (bare~~ containing particles are mixed with non-refractory material (pure rBC was not observed). There are also studies where rBC containing particles have disintegrated in the laser beam, which has been interpreted either as a result of very thick ~~coatings~~ non-refractory coatings around rBC cores (Dahlkötter et al., 2014) or that the rBC is attached to the surface or is close to the surface of a non-absorbing particle (Sedlacek et al., 2012; Moteki et al., 2014), but such behavior was not observed at Pallas.

3.2.2 Diurnal variations

~~Due to the high variability of the rBC parameters, statistically~~ Statistically significant diurnal cycles were not observed (not shown)~~. This~~ , which is not surprising as diurnal variations of solar radiation and temperature are minimal during the Arctic winter. However, when diurnal cycles are calculated

separately for the polar night and the following early spring, weak diurnal cycles can be observed in rBC mass concentration, but not in the other aerosol parameters (rBC core diameter and mixing state). During the polar night, rBC mass concentration peaks during midnight, which could ~~refer to~~ indicate regional emissions. After the polar night, rBC concentration has the maximum during local midday followed by an afternoon decrease, which can be explained by dilution when the mixing layer height increases. In general, other factors such as source region and removal processes during the transport time are more important for the variability of both rBC mass and mixing state parameters especially during winter.

3.3 Correlation with other observations

Most of the rBC parameters have rapid variations (see Fig. 3) compared with the time scales of variations of the observed trace gas concentrations (CO, CO_2, NO_2, SO_2 and O_3), meteorological parameters (temperature, pressure, and wind direction and speed) and computed backward trajectories (total length and average direction, distance and altitude). However, at least rBC mass concentration trends can be correlated with certain trace gases and trajectory ~~or wind~~ (or wind) directions. The other parameters ~~such as~~ (rBC geometric mass mean diameter, number fraction and ~~coating thickness seemed to~~ particle to rBC core diameter ratio) seem to be less dependent on the ~~weather~~ meteorological and trajectory parameters and concentrations of the trace gases.

From the trace gases, the best correlations are seen between rBC mass and CO, NO_2 and CO_2 concentrations (Pearson's correlation coefficients are between 0.61 and 0.76) as these are co-emitted during different combustion processes. ~~Carbon~~ Pearson's correlation coefficients for the other rBC parameters (mean diameter and mixing state) and the trace gases are between -0.35 and 0.42, which means weak or no correlation. Here we focus on the correlation between rBC mass concentration and carbon monoxide (CO), which is the most commonly used tracer~~, so we will focus on that.~~. Concentration time series of CO is shown in Fig. 3 and Fig. 4 shows the correlation between rBC and CO and a linear fit to the data. Pearson's correlation coefficient for ~~a linear fit between rBC and CO~~ the fit is 0.74, slope $\Delta\mathrm{rBC}/\Delta\mathrm{CO}$ is 0.742 $\mathrm{ng\,m^{-3}\,ppb^{-1}}$ ($\mathrm{ppb} = \mathrm{nmol\,mol^{-1}}$) and the offset is -93 $\mathrm{ng\,m^{-3}}$. Solving the background CO concentration (CO concentration where rBC concentration is zero) ~~is~~ from the fitted slope and offset gives 126 ppb. $\Delta\mathrm{rBC}/\Delta\mathrm{CO}$ values depend on the aerosol source and the age of the air mass (e.g., McMeeking et al., 2012). Current $\Delta\mathrm{rBC}/\Delta\mathrm{CO}$ value is lower than that from most other SP2 studies focusing on fresh biomass burning, industrial and urban plumes ~~(e.g., McMeeking et al., 2010; Kondo et al., 2011; Baumgardner et al., 2007; McMeeking et al., 2012; Sahu et al., 2012)~~ (e.g., Spackman et al., 2008; McMeeking et al., 2010; Kondo et al., 2011; Baumgardner et al., 2007; McMeeking et al., 2012; Sahu
Instead of having different rBC and CO sources, the low $\Delta\mathrm{rBC}/\Delta\mathrm{CO}$ value observed at Pallas is more likely the result of aging of the air masses during the transport from source regions to Pallas. The ratio decreases during the transport due to the extended CO lifetime (low levels of solar radiation) and efficient removal of the relatively hydrophilic ~~thickly coated~~ aged rBC during the

rainy and cloudy winter months. Similar and even lower ΔrBC/ΔCO values have been observed in free troposphere background air and in air masses that have been experiencing heavy precipitation ~~(Liu et al., 2010; Matsui et al., 2011).~~ (Liu et al., 2010; Matsui et al., 2011; Taylor et al., 2014). As can be seen from Fig. 4, the values cover a relatively wide range around the linear fit. This variability does not show clear dependence on the available trajectory, meteorological or rBC mixing state parameters. As an example, the marker color shows the particle to rBC core diameter ratio for each data point. Although the higher diameter ratios seem to be mostly above the linear fit, these are not clearly separated from the other data points.

It is assumed that the calculated average trajectory directions (time series shown in Fig. 3) describe the origin of air masses better than the measured local wind directions. Therefore, Fig. 5 shows rBC mass concentration (here 3 h averages) as a function of average trajectory direction. The trajectory directions can be divided into three source regions: Arctic Ocean, Continental Europe and North Atlantic. ~~Each data point is also~~ The other trajectory parameters (total length and average altitude and distance) were also examined and it seems that especially the average distance can explain some variations in the observed rBC concentrations, but these are less dependent on the total length and practically independent of the average altitude. Therefore, each data point in Fig. 5 is colored based on the average ~~trajectory distance~~ distance given as kilometers from the measurement location. In good agreement with the expectations, the figure shows that rBC concentrations are low when air masses are originating from North Atlantic or Arctic Ocean, and the highest concentrations are observed when trajectories are originating from the southern sector and especially from Eastern Europe (average distance more than 1000 km). The lowest concentrations in this polluted sector are observed when air masses are originating mainly from Southern Finland and the Baltic Countries (average distance less than 1000 km). Again, rBC ~~number fractions and coating thicknesses~~ mixing state and the other size distribution parameters seemed to be independent of air mass origin ~~.~~ ~~Especially coating thickness~~ (total length or average direction, distance or altitude). Especially the fraction of non-refractory material could have been dependent on rBC source region (age), which was not observed, but it is possible that this data set is too short for finding such dependencies.

It seems that from the rBC mixing state and size distribution parameters only the rBC mass concentration is clearly correlated with air mass origin described by trajectories and trace gas concentrations. One reason for the lack of correlations for the other parameters is that these have relatively low variations compared with that of rBC mass concentration. In addition, the variations seem to have shorter time scales (day-to-day variations) compared with those of the trajectories and trace gas concentrations (Fig. 3).

3.4 Refractory and equivalent black carbon

MAAP and Aethalometer use optical methods to measure aerosol absorption coefficients which are converted to equivalent BC (eBC) mass concentrations. Figure 6 shows correlations between these

two and rBC concentration measured by the SP2. The Aethalometer and MAAP eBC concentrations are in good agreement when the Pallas measurement site is not in cloud (circled data points). During the in cloud conditions and when the presence of clouds is unclear, the PM_{10} (humid size) eBC measured by MAAP is 30–100 % of the total eBC measured by the Aethalometer; similar decrease is also expected for the rBC mass concentration measured by the SP2 during in cloud conditions. PM_{10} and total eBC concentrations can be similar during the in cloud conditions if ~~ice particle and cloud droplet sizes~~ most cloud droplets are smaller than 10 µm~~or~~, other than eBC containing particles have been activating or the number fraction of activated particles is low.

The rBC is about 20 % of the eBC measured by MAAP (both PM_{10}), but the fraction is practically constant. This indicates that the difference is not caused by the time dependent aerosol properties such as mixing state. The factor of five difference between eBC and rBC is ~~unexpected, but smaller differences are possible. For example, our unpublished laboratory experiments with this same SP2 have shown a factor of two difference for Aquadag® aerosol. There are several~~ significantly larger than could be explained by typical measurement uncertainties (see the Instrumentation section), but there are other potential reasons for the observed difference. First of all, ~~rBC is a fraction of eBC , which can contain non-refractory~~ eBC detected by MAAP can contain light absorbing organics ~~such~~ generally referred as brown carbon ~~. Secondly, MAAP detects practically all absorbing particles, but~~ (e.g. Bond et al., 2013). Since brown carbon is typically non-refractory and weakly absorbing at the near-infrared wavelengths, it cannot be detected by the SP2. However, brown carbon absorption should have a strong wavelength dependency, but this is not seen in the Aethalometer data: the average absorption Ångström exponent for wavelengths from 370 nm to 950 nm is 1.2, which is a typical value for black carbon coated with non-absorbing material (Lack and Langridge, 2013). This indicates that brown carbon alone cannot explain the difference between eBC and rBC. Secondly, SP2 sizing is limited to 75–655 nm rBC core volume equivalent diameter range. Although larger rBC particles, which ~~saturate the incandescence detectors~~can be detected but not sized, were rarely observed, rBC particles smaller than 75 nm can also have a non-negligible mass. ~~Third, thick non-refractory coatings can increase absorption and MAAP eBC mass due to the lensing effect, but~~ Although the limited sizing range of the SP2 ~~results are independent of the coatings (Slowik et al., 2007). Fourth~~can explain a few time periods with low rBC concentration, is not likely explanation for the whole campaign. Third, these instruments have composition dependent parameters (mass absorption coefficient (MAC) for MAAP and incandescence efficiencies of the calibration and ambient rBC for SP2), which currently unknown optimal values might differ from the used default values. For example, accumulation of non-refractory material (both internally and externally mixed) to the filter can increase absorption measured by MAAP (Slowik et al., 2007; Cappa et al., 2008), which could be accounted for by increasing MAC. Default MAC ($6.6\,m^2\,g^{-1}$) was used in Pallas MAAP data analysis, but larger values up to factor of two have been reported ~~(e.g., Liu et al., 2010; Lack et al., 2014)~~(e.g., Liu et al., 2010; Bond et al., 2013; Lack et al., 2014).

Current SP2 was calibrated using Aquadag®, but using a specific batch of fullerene soot which represents ambient aerosol in Tokyo (Moteki and Kondo, 2010) as a calibration material would have given about 33 % larger rBC mass ~~for the same measured incandescence signal (Laborde et al., 2012b, a). Although these instrument parameters can explain a large fraction of the factor of five differences~~ (Laborde et al., 2012b, a). Using the default MAC for the MAAP and Aquadag® calibration for the SP2 could explain a part of the difference between eBC and rBC~~, it is likely that some fraction of the total absorbing aerosol mass in Pallas is non-refractory material such as brown carbon~~ . However, the default MAC and Aquadag® have been used successfully in several studies, so it is unlikely that a bias in these could fully explain the observed factor of five difference. It is therefore possible that a part of the difference is caused the presence of brown carbon or more generally a light absorbing carbon with high volatility or low absorption at the wavelength used by the SP2.

3.5 Climate implications

Several studies have been using numerical models to quantify the effects of black carbon mixing state on aerosol radiative properties and climate (e.g. Bond and Bergstrom, 2006; Adachi et al., 2010; Bond et al., 2013), however, most of these studies are made without detailed experimental information about the mixing state that can be obtained from single particle instruments such as the SP2. In this section we ~~will quantify the effect of~~ compare the effects of different black carbon mixing state representations on aerosol radiative properties ~~when the total aerosol composition is known (from~~ and climate when the models are constrained by our measurements described in the previous sections~~)~~. From the various mixing state representations (see e.g., Lang-Yona et al., 2010), we have selected ~~the one that matches~~ two that match with the current observations and ~~four~~ three other that are in common use. The five mixing state representations include two internally mixed (only one particle type containing both absorbing and non-absorbing material) and three externally mixed (separate absorbing and non-absorbing particle types) aerosol populations. The internally mixed particles can be homogenous (INT-HOM) or absorbing cores with a non-absorbing coating (INT-COAT). The externally mixed particles have always one non-absorbing and one absorbing ~~size distribution~~particle type. The absorbing particles can be bare absorbing material (EXT-BARE), coated absorbing cores (EXT-COAT) or a homogenous mixture of the absorbing and non-absorbing components (EXT-HOM). ~~The~~ Particle structures cannot be directly measured by the SP2, but single particle imaging studies have shown that aged ambient particles are typically composed of a compact black carbon cluster mixed with non-absorbing material, which is often described by a homogenous particle or a coated black carbon core model (e.g. Bond et al., 2013). If it is assumed that the black carbon forms a distinct core then the EXT-COAT case is the one ~~based on our observations~~closest to our observations, but otherwise EXT-HOM case is more appropriate.

All model calculations are based on the same total particle size distribution and chemical composition (campaign averages), but the absorbing and non-absorbing species are distributed differently ~~according to the~~ in each mixing state representation. Based on our measurements, the average total rBC mass concentration is 26 $\mathrm{ng\,m^{-3}}$, the number fraction of particles containing rBC is 0.24 and ~~coated to (refractory)~~ particle to rBC core diameter ratio is 2.0. This means that the total rBC volume fraction is ~~(~~$0.24/2.0^3$ ~~=)~~ 0.03 and the rest is non-refractory material. Also, the total volume of all particles must be $460 \times 10^{-9}\,\mathrm{cm^3\,m^{-3}}$ based on the observed rBC mass concentration (density is $1800\,\mathrm{kg\,m^{-3}}$) and volume fraction (0.03). Because SP2 does not detect scattering particles smaller than 190 nm, particle size distribution parameters are obtained from the gas line DMPS measurements: geometric volume mean diameter and standard deviation are 323 nm and 1.54, respectively. Volume distribution is used here, because particles larger than 100 nm have the dominant effect on light absorption and scattering. As described in Sect. 3.4, ~~significant fraction of the absorbing material is likely to be non-refractory. Therefore, the absorbing component of the~~ refractory black carbon (rBC) detected by the SP2 is only about 20 % of the equivalent black carbon (eBC) measured by the MAAP. Here we assume that the difference is caused by the presence of non-refractory ~~material is here considered as light absorbing~~ light absorbing organic carbon (LAC) ~~and it's volume fraction is calculated from that of the eBC (eBC = rBC + LAC) measured by the MAAP~~which cannot be detected by the SP2. Based on the average rBC to eBC ratio of 0.21, eBC volume fraction is 0.15 ~~, which means that~~ and the LAC volume fraction is 0.12 (eBC = rBC + LAC). The rest of the total volume is assumed to be ammonium sulfate. Optical constants of the different particle types are calculated as a volume fraction weighted average of those of the pure compounds. The complex refractive indices of ammonium sulfate, LAC and rBC are $1.51 + 0i$, $1.95 + 0.79i$ Baumgardner et al. (2007) and $2.26 + 1.26i$ (Moteki et al., 2010), respectively. ~~For example, in~~ Simple illustration of the five different mixing state representations is shown in Fig. 7. In the EXT-COAT case, 24 % of the particles ~~contain absorbing material and the rest are pure~~ are absorbing and the remaining 76 % are composed of non-absorbing ammonium sulfate. The absorbing particles contain a core, which is composed of a mixture of rBC ($1/2.0^3$ of the particle volume) and LAC ($0.12/0.03 \cdot 1/2.0^3$ of the particle volume), and the coating is ammonium sulfate. The EXT-HOM case is similar to that except that the absorbing particles are homogeneous mixtures of the three components. The EXT-BARE case has the same total amount of absorbing material, which means that the absorbing particle number fraction is the same as the total absorbing volume fraction. The INT-HOM and INT-COAT cases are constructed so that the absorbing volume fraction in each particle is the same as the total absorbing volume fraction.

Numerical calculations using the Bohren and Huffman (1983) BHMIE and BHCOAT codes give extinction (b_{ext}) and absorption coefficients (b_{abs}) and backscatter fraction (b) for the particle populations at 550 nm wavelength. These are the main parameters in an equation for global mean top of atmosphere radiative forcing efficiency (RFE) per unit optical depth (Haywood and Shine, 1995;

Anderson et al., 1999):

$$\mathrm{RFE} = SD(1-A_\mathrm{c})T_\mathrm{a}^2(1-R_\mathrm{s})^2\left(\frac{2R_\mathrm{s}(1-\omega)}{(1-R_\mathrm{s})^2}-\beta\omega\right) \quad (1)$$

The parameters are solar constant ($S = 1370\,\mathrm{W\,m^{-2}}$), annual average daylight fraction ($D = 0.5$), fractional cloud coverage ($A_\mathrm{c} = 0.6$), atmospheric transmissivity ($T_\mathrm{a} = 0.87$), surface albedo (R_s=0.2), single scattering albedo ($\omega = 1 - b_\mathrm{abs}/b_\mathrm{ext}$), and average upscatter fraction (β). The upscatter fraction is parameterized as a function of backscatter fraction b: $\beta = 0.082 + 1.85b - 2.97b^2$ (Anderson et al., 1999). Although Eq. (1) is highly simplified solution for a complex problem and its parameters have uncertainties, which means that the absolute RFE values are not fully accurate, this equation is suitable for comparing different mixing state models.

The results of the calculations, which include extinction and absorption coefficients and backscatter fraction used in Eq. (1), are given in Table 1. Because the absorbing material is distributed over all particles in the internally mixed aerosol~~particles~~, which means larger effective absorption cross section, this aerosol is more absorbing and less scattering than the externally mixed aerosol ~~(e.g., Cappa et al., 2012). Compared with the overall difference between the internally and externally mixed aerosol, the difference between core-shell and homogenous particle types is small.~~ where only a fraction particles are absorbing (e.g., Cappa et al., 2012). Mainly due to the differences in single scattering albedo, RFE values are positive (warming effect) for the internally mixed aerosol and negative (cooling effect) for the externally mixed aerosol. As the current and most other experimental results show that at least the aged rBC aerosol population is externally mixed, assuming an ~~internal mixture~~ internally mixed aerosol would lead to overestimated climate warming effect. Compared with the overall difference in RFE between the internally and externally mixed absorbing aerosol populations, the effect of single particle structure on RFE is small. This means that at least in this case the number fraction of absorbing particles is more important for the aerosol radiative forcing than the exact single particle structure.

4 Conclusions

We have measured refractory black carbon (rBC) mass distributions and mixing state by using a Single Particle Soot Photometer (SP2) at an Arctic measurement site in Northern Finland. To our knowledge, these are the first published surface SP2 measurements made in the Fennoscandian Arctic. The results show that rBC mass concentrations are relatively low (average mass concentration $26\,\mathrm{ng\,m^{-3}}$) and most of the rBC is long-range transported from south. Observed ~~particles are larger~~ rBC core sizes (geometric mass mean diameter 194 nm) ~~than those observed close to the source regions~~are typical for aged air masses. On the average, 24 % of the accumulation mode particles contain an observable (volume equivalent diameter at least 75 nm) rBC core. These particles ~~are thickly coated~~ contain large fractions of non-refractory material with the average ~~coated to~~ particle

to rBC core diameter ratio 2.0; bare rBC particles or other than ~~core-shell structures~~ mixed particle structures (e.g. rBC attached to non-absorbing particles) were not observed.

From the rBC mass ~~distributions~~ distribution and mixing state parameters only the mass concentration was clearly correlated with certain co-emitted trace gases~~including carbon monoxide (CO), carbon dioxide (CO_2) and nitrogen dioxide (NO_2)~~. The correlation of rBC with ~~CO~~ carbon monoxide (CO) showed shallow slope, which was interpreted as a result of relatively aged air masses where rBC has been removed mainly by wet deposition. Similarly, rBC mass concentration was also the only parameter that correlated with air mass history described by the average directions and lengths of backward trajectories. The largest concentrations were observed when the trajectories were originating from Eastern Europe and the lowest concentrations were from North Atlantic and Arctic Ocean.

SP2 measurements provided detailed information about the rBC mixing state, but ~~different mixing states have been~~ the observations are not always in agreement with the mixing state representations used in various aerosol models. The ~~effect of rBC~~ effects of absorbing aerosol mixing state on aerosol radiative properties were estimated by using a Mie approximation and a simple direct radiative forcing efficiency calculations. The difference between ~~core-shell and homogenous particle structures~~ single particle structures (e.g. absorbing core coated with non-absorbing material or homogenous absorbing particle) is small compared with that between internally (all particles ~~have an absorbingcomponent~~are absorbing) and externally (a fraction of particles ~~have an absorbingcomponent) mixed~~ are absorbing) mixed absorbing aerosol populations. The internally mixed aerosol population is more absorbing due to the higher effective absorbing cross sectional area, which means that these aerosols are more likely to have a warming effect. However, the same aerosol can have a cooling effect when assuming externally mixed absorbing and non-absorbing particles. Our current and most other observations show that especially the aged ~~absorbing~~ aerosol is externally mixed~~(a fraction of particles are absorbing)~~, which means that assuming an internally mixed homogenous aerosol means overestimated aerosol warming effect.

Current radiative forcing calculations are highly simplified, so more detailed model calculations should be done to obtain a more realistic radiative forcing estimate. Before that can be done, accurate measurements are needed to develop a global picture of the mixing state of the absorbing aerosol. Long term measurements are also needed to observe the diurnal and annual cycles. SP2 is probably the best instrument for that purpose, but this requires consistent use of data analysis methods and reference materials.

Acknowledgements. This work was supported by the EU LIFE+ project MACEB (project no. LIFE09 ENV/FI/000572), the Academy of Finland project Greenhouse gas, aerosol and albedo variations in the changing Arctic (project number 269095), the Academy of Finland through the FCoE in Physics, Chemistry, Biology and Meteorology of Atmospheric Composition and Climate Change (program numbers 1118615 and 272041),

black and brown carbon influence on climate and climate change in India – from local to regional scale (project no. 264242), Arctic Absorbing Aerosols and Albedo of Snow (project no. 3162), the Nordic research and innovation initiative CRAICC, and KONE foundation. We would also like to thank J. Hatakka and T. Laurila for providing the gas data.

References

Adachi, K., Chung, S. H., and Buseck, P. R.: Shapes of soot aerosol particles and implications for their effects on climate, J. Geophys. Res., 115, D15206, doi:10.1029/2009JD012868, 2010.

Anderson, T. L., Covert, D. S., Wheeler, J. D., Harris, J. M., Perry, K. D., Trost, B. E., Jaffe, D. J., and Ogren, J. A.: Aerosol backscatter fraction and single scattering albedo: Measured values and uncertainties at a coastal station in the Pacific Northwest, J. Geophys. Res., 104, 26793–26807, 1999.

Baumgardner, D., Kok, G., and Raga, G.: Warming of the Arctic lower stratosphere by light absorbing particles, Geophys. Res. Lett., 31, L06117, doi:10.1029/2003GL018883, l06117, 2004.

Baumgardner, D., Kok, G. L., and Raga, G. B.: On the diurnal variability of particle properties related to light absorbing carbon in Mexico City, Atmos. Chem. Phys., 7, 2517–2526, doi:10.5194/acp-7-2517-2007, 2007.

Baumgardner, D., Popovicheva, O., Allan, J., Bernardoni, V., Cao, J., Cavalli, F., Cozic, J., Diapouli, E., Eleftheriadis, K., Genberg, P. J., Gonzalez, C., Gysel, M., John, A., Kirchstetter, T. W., Kuhlbusch, T. A. J., Laborde, M., Lack, D., Müller, T., Niessner, R., Petzold, A., Piazzalunga, A., Putaud, J. P., Schwarz, J., Sheridan, P., Subramanian, R., Swietlicki, E., Valli, G., Vecchi, R., and Viana, M.: Soot reference materials for instrument calibration and intercomparisons: a workshop summary with recommendations, Atmos. Meas. Tech., 5, 1869–1887, doi:10.5194/amt-5-1869-2012, 2012.

Bohren, C. and Huffman, D. R.: Absorption and scattering of light by small particles, Wiley, New York, 1983.

Bond, T. C. and Bergstrom, R. W.: Light Absorption by Carbonaceous Particles: An Investigative Review, Aerosol Sci. Tech., 40, 27–67, doi:10.1080/02786820500421521, 2006.

Bond, T. C., Doherty, S. J., Fahey, D. W., Forster, P. M., Berntsen, T., DeAngelo, B. J., Flanner, M. G., Ghan, S., Kärcher, B., Koch, D., Kinne, S., Kondo, Y., Quinn, P. K., Sarofim, M. C., Schultz, M. G., Schulz, M., Venkataraman, C., Zhang, H., Zhang, S., Bellouin, N., Guttikunda, S. K., Hopke, P. K., Jacobson, M. Z., Kaiser, J. W., Klimont, Z., Lohmann, U., Schwarz, J. P., Shindell, D., Storelvmo, T., Warren, S. G., and Zender, C. S.: Bounding the role of black carbon in the climate system: A scientific assessment, J. Geophys. Res., 118, 5380–5552, doi:10.1002/jgrd.50171, 2013.

Cappa, C. D., Lack, D. A., Burkholder, J. B., and Ravishankara, A. R.: Bias in Filter-Based Aerosol Light Absorption Measurements Due to Organic Aerosol Loading: Evidence from Laboratory Measurements, Aerosol Sci. Tech., 42, 1022–1032, doi:10.1080/02786820802389285, 2008.

Cappa, C. D., Onasch, T. B., Massoli, P., Worsnop, D. R., Bates, T. S., Cross, E. S., Davidovits, P., Hakala, J., Hayden, K. L., Jobson, B. T., Kolesar, K. R., Lack, D. A., Lerner, B. M., Li, S.-M., Mellon, D., Nuaaman, I., Olfert, J. S., Petäjä, T., Quinn, P. K., Song, C., Subramanian, R., Williams, E. J., and Zaveri, R. A.: Radiative Absorption Enhancements Due to the Mixing State of Atmospheric Black Carbon, Science, 337, 1078–1081, doi:10.1126/science.1223447, 2012.

Dahlkötter, F., Gysel, M., Sauer, D., Minikin, A., Baumann, R., Seifert, P., Ansmann, A., Fromm, M., Voigt, C., and Weinzierl, B.: The Pagami Creek smoke plume after long-range transport to the upper troposphere over Europe – aerosol properties and black carbon mixing state, Atmos. Chem. Phys., 14, 6111-6137, doi:10.5194/acp-14-6111-2014, 2014.

Draxler, R.: HYSPLIT4 user's guide, NOAA Tech. Memo. ERL ARL-230, NOAA Air Resources Laboratory, Silver Spring, MD, 1999.

Draxler, R. and Hess, G.: Description of the HYSPLIT_4 modeling system., NOAA Tech. Memo. ERL ARL-224, NOAA Air Resources Laboratory, Silver Spring, MD, 24 pp., 1997.

Draxler, R. and Hess, G.: An overview of the HYSPLIT_4 modeling system of trajectories, dispersion, and deposition, Aust. Meteorol. Mag., 47, 295–308, 1998.

Dutkiewicz, V. A., DeJulio, A. M., Ahmed, T., Laing, J., Hopke, P. K., Skeie, R. B., Viisanen, Y., Paatero, J., and Husain, L.: Forty-seven years of weekly atmospheric black carbon measurements in the Finnish Arctic: Decrease in black carbon with declining emissions, J. Geophys. Res., 119, 7667–7683, doi:10.1002/2014JD021790, 2014.

Flanner, M. G., Zender, C. S., Randerson, J. T., and Rasch, P. J.: Present-day climate forcing and response from black carbon in snow, J. Geophys. Res., 112, D11202, doi:10.1029/2006JD008003, 2007.

Gao, R. S., Schwarz, J. P., Kelly, K. K., Fahey, D. W., Watts, L. A., Thompson, T. L., Spackman, J. R., Slowik, J. G., Cross, E. S., Han, J.-H., Davidovits, P., Onasch, T. B., and Worsnop, D. R.: A Novel Method for Estimating Light-Scattering Properties of Soot Aerosols Using a Modified Single-Particle Soot Photometer, Aerosol Sci. Tech., 41, 125–135, doi:10.1080/02786820601118398, 2007.

Genberg, J., Denier van der Gon, H. A. C., Simpson, D., Swietlicki, E., Areskoug, H., Beddows, D., Ceburnis, D., Fiebig, M., Hansson, H. C., Harrison, R. M., Jennings, S. G., Saarikoski, S., Spindler, G., Visschedijk, A. J. H., Wiedensohler, A., Yttri, K. E., and Bergström, R.: Light-absorbing carbon in Europe – measurement and modelling, with a focus on residential wood combustion emissions, Atmos. Chem. Phys., 13, 8719–8738, doi:10.5194/acp-13-8719-2013, 2013.

Gysel, M., Laborde, M., Olfert, J. S., Subramanian, R., and Gröhn, A. J.: Effective density of Aquadag and fullerene soot black carbon reference materials used for SP2 calibration, Atmos. Meas. Tech., 4, 2851–2858, doi:10.5194/amt-4-2851-2011, 2011.

Hansen, A., Rosen, H., and Novakov, T.: The aethalometer – An instrument for the real-time measurement of optical absorption by aerosol particles, Sci. Total Environ., 36, 191–196, doi:10.1016/0048-9697(84)90265-1, 1984.

Hansen, J. and Nazarenko, L.: Soot climate forcing via snow and ice albedos, P. Natl. Acad. Sci. USA, 101, 423–428, doi:10.1073/pnas.2237157100, 2004.

Hatakka, J., Aalto, T., Aaltonen, V., Aurela, M., Hakola, H., Komppula, M., Laurila, T., Lihavainen, H., Paatero, J., Salminen, K., and Viisanen, Y.: Overview of the atmospheric research activities and results at Pallas GAW station, Boreal Environ. Res., 8, 365–383, 2003.

Haywood, J. M. and Shine, K. P.: The effect of anthropogenic sulfate and soot aerosol on the clear sky planetary radiation budget, Geophys. Res. Lett., 22, 603–606, doi:10.1029/95GL00075, 1995.

Huang, X.-F., Sun, T.-L., Zeng, L.-W., Yu, G.-H., and Luan, S.-J.: Black carbon aerosol characterization in a coastal city in South China using a single particle soot photometer, Atmos. Environ., 51, 21–28, 2012.

Hyvärinen, A.-P., Kolmonen, P., Kerminen, V.-M., Virkkula, A., Leskinen, A., Komppula, M., Hatakka, J., Burkhart, J., Stohl, A., Aalto, P., Kulmala, M., Lehtinen, K., Viisanen, Y., and Lihavainen, H.: Aerosol black carbon at five background measurement sites over Finland, a gateway to the Arctic, Atmos. Environ., 45, 4042–4050, 2011.

Kipling, Z., Stier, P., Schwarz, J. P., Perring, A. E., Spackman, J. R., Mann, G. W., Johnson, C. E., and Telford, P. J.: Constraints on aerosol processes in climate models from vertically-resolved aircraft observations of black carbon, Atmos. Chem. Phys., 13, 5969–5986, doi:10.5194/acp-13-5969-2013, 2013.

Komppula, M., Lihavainen, H., Kerminen, V.-M., Kulmala, M., and Viisanen, Y.: Measurements of cloud droplet activation of aerosol particles at a clean subarctic background site, J. Geophys. Res., 110, D06204, doi:10.1029/2004JD005200, 2005.

Kondo, Y., Matsui, H., Moteki, N., Sahu, L., Takegawa, N., Kajino, M., Zhao, Y., Cubison, M. J., Jimenez, J. L., Vay, S., Diskin, G. S., Anderson, B., Wisthaler, A., Mikoviny, T., Fuelberg, H. E., Blake, D. R., Huey, G., Weinheimer, A. J., Knapp, D. J., and Brune, W. H.: Emissions of black carbon, organic, and inorganic aerosols from biomass burning in North America and Asia in 2008, J. Geophys. Res., 116, D08204, doi:10.1029/2010JD015152, 2011.

Laborde, M., Mertes, P., Zieger, P., Dommen, J., Baltensperger, U., and Gysel, M.: Sensitivity of the Single Particle Soot Photometer to different black carbon types, Atmos. Meas. Tech., 5, 1031–1043, doi:10.5194/amt-5-1031-2012, 2012a.

Laborde, M., Schnaiter, M., Linke, C., Saathoff, H., Naumann, K.-H., Möhler, O., Berlenz, S., Wagner, U., Taylor, J. W., Liu, D., Flynn, M., Allan, J. D., Coe, H., Heimerl, K., Dahlkötter, F., Weinzierl, B., Wollny, A. G., Zanatta, M., Cozic, J., Laj, P., Hitzenberger, R., Schwarz, J. P., and Gysel, M.: Single Particle Soot Photometer intercomparison at the AIDA chamber, Atmos. Meas. Tech., 5, 3077–3097, doi:10.5194/amt-5-3077-2012, 2012b.

Lack, D. A. and Langridge, J. M.: On the attribution of black and brown carbon light absorption using the Ångström exponent, Atmos. Chem. Phys., 13, 10535–10543, doi:10.5194/acp-13-10535-2013, 2013.

Lack, D., Moosmüller, H., McMeeking, G., Chakrabarty, R., and Baumgardner, D.: Characterizing elemental, equivalent black, and refractory black carbon aerosol particles: a review of techniques, their limitations and uncertainties, Anal. Bioanal. Chem., 406, 99–122, doi:10.1007/s00216-013-7402-3, 2014.

Lang-Yona, N., Abo-Riziq, A., Erlick, C., Segre, E., Trainic, M., and Rudich, Y.: Interaction of internally mixed aerosols with light, Phys. Chem. Chem. Phys., 12, 21–31, doi:10.1039/B913176K, 2010.

Lihavainen, H., Hyvärinen, A., Asmi, E., Hatakka, J., and Viisanen, Y.: Long-term variability of aerosol optical properties in northern Finland, Boreal Env. Res., 20, 526–541, 2015.

Liu, D., Flynn, M., Gysel, M., Targino, A., Crawford, I., Bower, K., Choularton, T., Jurányi, Z., Steinbacher, M., Hüglin, C., Curtius, J., Kampus, M., Petzold, A., Weingartner, E., Baltensperger, U., and Coe, H.: Single particle characterization of black carbon aerosols at a tropospheric alpine site in Switzerland, Atmos. Chem. Phys., 10, 7389–7407, doi:10.5194/acp-10-7389-2010, 2010.

Liu, D., Allan, J., Whitehead, J., Young, D., Flynn, M., Coe, H., McFiggans, G., Fleming, Z. L., and Bandy, B.: Ambient black carbon particle hygroscopic properties controlled by mixing state and composition, Atmos. Chem. Phys., 13, 2015–2029, doi:10.5194/acp-13-2015-2013, 2013.

Matsui, H., Kondo, Y., Moteki, N., Takegawa, N., Sahu, L. K., Zhao, Y., Fuelberg, H. E., Sessions, W. R., Diskin, G., Blake, D. R., Wisthaler, A., and Koike, M.: Seasonal variation of the transport of black carbon aerosol from the Asian continent to the Arctic during the ARCTAS aircraft campaign, J. Geophys. Res., 116, D05202, doi:10.1029/2010JD015067, 2011.

McMeeking, G. R., Hamburger, T., Liu, D., Flynn, M., Morgan, W. T., Northway, M., Highwood, E. J., Krejci, R., Allan, J. D., Minikin, A., and Coe, H.: Black carbon measurements in the boundary layer over western and northern Europe, Atmos. Chem. Phys., 10, 9393–9414, doi:10.5194/acp-10-9393-2010, 2010.

McMeeking, G. R., Bart, M., Chazette, P., Haywood, J. M., Hopkins, J. R., McQuaid, J. B., Morgan, W. T., Raut, J.-C., Ryder, C. L., Savage, N., Turnbull, K., and Coe, H.: Airborne measurements of trace gases and aerosols over the London metropolitan region, Atmos. Chem. Phys., 12, 5163–5187, doi:10.5194/acp-12-5163-2012, 2012.

Metcalf, A. R., Craven, J. S., Ensberg, J. J., Brioude, J., Angevine, W., Sorooshian, A., Duong, H. T., Jonsson, H. H., Flagan, R. C., and Seinfeld, J. H.: Black carbon aerosol over the Los Angeles Basin during CalNex, J. Geophys. Res., 117, D00V13, doi:10.1029/2011JD017255, 2012.

Moteki, N. and Kondo, Y.: Dependence of Laser-Induced Incandescence on Physical Properties of Black Carbon Aerosols: Measurements and Theoretical Interpretation, Aerosol Sci. Tech., 44, 663–675, doi:10.1080/02786826.2010.484450, 2010.

Moteki, N., Kondo, Y., Miyazaki, Y., Takegawa, N., Komazaki, Y., Kurata, G., Shirai, T., Blake, D. R., Miyakawa, T., and Koike, M.: Evolution of mixing state of black carbon particles: Aircraft measurements over the western Pacific in March 2004, Geophys. Res. Lett., 34, L11803, doi:10.1029/2006GL028943, 2007.

Moteki, N., Kondo, Y., and Nakamura, S.: Method to measure refractive indices of small nonspherical particles: Application to black carbon particles, J. Aerosol Sci., 41, 513–521, 2010.

Moteki, N., Kondo, Y., and Adachi, K.: Identification by single-particle soot photometer of black carbon particles attached to other particles: Laboratory experiments and ground observations in Tokyo, J. Geophys. Res., 119, 1031–1043, doi:10.1002/2013JD020655, 2014.

Petzold, A. and Schönlinner, M.: Multi-angle absorption photometry – a new method for the measurement of aerosol light absorption and atmospheric black carbon, J. Aerosol Sci., 35, 421–441, doi:10.1016/j.jaerosci.2003.09.005, 2004.

Petzold, A., Ogren, J. A., Fiebig, M., Laj, P., Li, S.-M., Baltensperger, U., Holzer-Popp, T., Kinne, S., Pappalardo, G., Sugimoto, N., Wehrli, C., Wiedensohler, A., and Zhang, X.-Y.: Recommendations for reporting "black carbon" measurements, Atmos. Chem. Phys., 13, 8365–8379, doi:10.5194/acp-13-8365-2013, 2013.

Reddington, C. L., McMeeking, G., Mann, G. W., Coe, H., Frontoso, M. G., Liu, D., Flynn, M., Spracklen, D. V., and Carslaw, K. S.: The mass and number size distributions of black carbon aerosol over Europe, Atmos. Chem. Phys., 13, 4917–4939, doi:10.5194/acp-13-4917-2013, 2013.

Sahu, L. K., Kondo, Y., Moteki, N., Takegawa, N., Zhao, Y., Cubison, M. J., Jimenez, J. L., Vay, S., Diskin, G. S., Wisthaler, A., Mikoviny, T., Huey, L. G., Weinheimer, A. J., and Knapp, D. J.: Emission characteristics of black carbon in anthropogenic and biomass burning plumes over California during ARCTAS-CARB 2008, J. Geophys. Res., 117, D16302, doi:10.1029/2011JD017401, 2012.

Samset, B. H., Myhre, G., Herber, A., Kondo, Y., Li, S.-M., Moteki, N., Koike, M., Oshima, N., Schwarz, J. P., Balkanski, Y., Bauer, S. E., Bellouin, N., Berntsen, T. K., Bian, H., Chin, M., Diehl, T., Easter, R. C., Ghan, S. J., Iversen, T., Kirkevåg, A., Lamarque, J.-F., Lin, G., Liu, X., Penner, J. E., Schulz, M., Seland, Ø., Skeie, R. B., Stier, P., Takemura, T., Tsigaridis, K., and Zhang, K.: Modelled black carbon radiative forcing and atmospheric lifetime in AeroCom Phase II constrained by aircraft observations, Atmos. Chem. Phys., 14, 12465–12477, doi:10.5194/acp-14-12465-2014, 2014.

Schwarz, J. P., Gao, R. S., Fahey, D. W., Thomson, D. S., Watts, L. A., Wilson, J. C., Reeves, J. M., Darbeheshti, M., Baumgardner, D. G., Kok, G. L., Chung, S. H., Schulz, M., Hendricks, J., Lauer, A., Kärcher, B., Slowik, J. G., Rosenlof, K. H., Thompson, T. L., Langford, A. O., Loewenstein, M., and Aikin, K. C.: Single-particle measurements of midlatitude black carbon and light-scattering aerosols from the boundary layer to the lower stratosphere, J. Geophys. Res., 111, D16207, doi:10.1029/2006JD007076, 2006.

Schwarz, J. P., Gao, R. S., Spackman, J. R., Watts, L. A., Thomson, D. S., Fahey, D. W., Ryerson, T. B., Peischl, J., Holloway, J. S., Trainer, M., Frost, G. J., Baynard, T., Lack, D. A., de Gouw, J. A., Warneke, C., and Del Negro, L. A.: Measurement of the mixing state, mass, and optical size of individual black carbon particles in urban and biomass burning emissions, Geophys. Res. Lett., 35, L13810, doi:10.1029/2008GL033968, 2008a.

Schwarz, J. P., Spackman, J. R., Fahey, D. W., Gao, R. S., Lohmann, U., Stier, P., Watts, L. A., Thomson, D. S., Lack, D. A., Pfister, L., Mahoney, M. J., Baumgardner, D., Wilson, J. C., and Reeves, J. M.: Coatings and their enhancement of black carbon light absorption in the tropical atmosphere, J. Geophys. Res., 113, D03203, doi:10.1029/2007JD009042, 2008b.

Schwarz, J. P., Samset, B. H., Perring, A. E., Spackman, J. R., Gao, R. S., Stier, P., Schulz, M., Moore, F. L., Ray, E. A., and Fahey, D. W.: Global-scale seasonally resolved black carbon vertical profiles over the Pacific, Geophys. Res. Lett., 40, 5542–5547, doi:10.1002/2013GL057775, 2013.

Sedlacek, A. J., Lewis, E. R., Kleinman, L., Xu, J., and Zhang, Q.: Determination of and evidence for non-core-shell structure of particles containing black carbon using the Single-Particle Soot Photometer (SP2), Geophys. Res. Lett., 39, L06802, doi:10.1029/2012GL050905, 2012.

Slowik, J. G., Cross, E. S., Han, J.-H., Davidovits, P., Onasch, T. B., Jayne, J. T., Williams, L. R., Canagaratna, M. R., Worsnop, D. R., Chakrabarty, R. K., Moosmüller, H., Arnott, W. P., Schwarz, J. P., Gao, R.-S., Fahey, D. W., Kok, G. L., and Petzold, A.: An Inter-Comparison of Instruments Measuring Black Carbon Content of Soot Particles, Aerosol Sci. Tech., 41, 295–314, doi:10.1080/02786820701197078, 2007.

Stephens, M., Turner, N., and Sandberg, J.: Particle identification by laser-induced incandescence in a solid-state laser cavity, Appl. Optics, 42, 3726–3736, doi:10.1364/AO.42.003726, 2003.

IPCC: Climate Change 2013: The Physical Science Basis. Contribution of Working Group I to the Fifth Assessment Report of the Intergovernmental Panel on Climate Change, edited by: Stocker, T. F., Qin, D., Plattner, G.-K., Tignor, M., Allen, S. K., Boschung, J., Nauels, A., Xia, Y., Bex, V., and Midgley, P., Cambridge University Press, Cambridge, United Kingdom and New York, NY, USA, 1535 pp., 2013.

Stohl, A., Klimont, Z., Eckhardt, S., Kupiainen, K., Shevchenko, V. P., Kopeikin, V. M., and Novigatsky, A. N.: Black carbon in the Arctic: the underestimated role of gas flaring and residential combustion emissions, Atmos. Chem. Phys., 13, 8833–8855, doi:10.5194/acp-13-8833-2013, 2013.

Spackman, J. R., Schwarz, J. P., Gao, R. S., Watts, L. A., Thomson, D. S., Fahey, D. W., Holloway, J. S., de Gouw, J. A., Trainer, M., and Ryerson, T. B.: Empirical correlations between black carbon aerosol and carbon monoxide in the lower and middle troposphere, Geophys. Res. Lett., 35, L19816, doi:10.1029/2008GL035237, 2008.

Svensson, J., Virkkula, A., Meinander, O., Kivekäs, N., Hannula, H.-R., Järvinen, O., Peltoniemi, J. I., Gritsevich, M., Heikkilä, A., Kontu, A., Hyvärinen, A.-P., Neitola, K., Brus, D., Dagsson-Waldhauserova, P., Anttila, K., Hakala, T., Kaartinen, H., Vehkamäki, M., de Leeuw, G., and Lihavainen, H.: Soot on snow

experiments: light-absorbing impurities effect on the natural snowpack, The Cryosphere Discuss., 9, 1227–1267, doi:10.5194/tcd-9-1227-2015, 2015.

Taylor, J. W., Allan, J. D., Allen, G., Coe, H., Williams, P. I., Flynn, M. J., Le Breton, M., Muller, J. B. A., Percival, C. J., Oram, D., Forster, G., Lee, J. D., Rickard, A. R., Parrington, M., and Palmer, P. I.: Size-dependent wet removal of black carbon in Canadian biomass burning plumes, Atmos. Chem. Phys., 14, 13 755–13 771, doi:10.5194/acp-14-13755-2014, 2014.

Taylor, J. W., Allan, J. D., Liu, D., Flynn, M., Weber, R., Zhang, X., Lefer, B. L., Grossberg, N., Flynn, J., and Coe, H.: Assessment of the sensitivity of core/shell parameters derived using the single-particle soot photometer to density and refractive index, Atmos. Meas. Tech., 8, 1701–1718, doi:10.5194/amt-8-1701-2015, 2015.

Wang, Q., Jacob, D. J., Spackman, J. R., Perring, A. E., Schwarz, J. P., Moteki, N., Marais, E. A., Ge, C., Wang, J., and Barrett, S. R. H.: Global budget and radiative forcing of black carbon aerosol: Constraints from pole-to-pole (HIPPO) observations across the Pacific, J. Geophys. Res., 119, 195–206, doi:10.1002/2013JD020824, 2014a.

Wang, X., Heald, C. L., Ridley, D. A., Schwarz, J. P., Spackman, J. R., Perring, A. E., Coe, H., Liu, D., and Clarke, A. D.: Exploiting simultaneous observational constraints on mass and absorption to estimate the global direct radiative forcing of black carbon and brown carbon, Atmos. Chem. Phys., 14, 10989–11010, doi:10.5194/acp-14-10989-2014, 2014b.

Weingartner, E., Saathoff, H., Schnaiter, M., Streit, N., Bitnar, B., and Baltensperger, U.: Absorption of light by soot particles: determination of the absorption coefficient by means of aethalometers, J. Aerosol Sci., 34, 1445–1463, 2003.

Zhang, R., Khalizov, A. F., Pagels, J., Zhang, D., Xue, H., and McMurry, P. H.: Variability in morphology, hygroscopicity, and optical properties of soot aerosols during atmospheric processing, P. Natl. Acad. Sci. USA, 105, 10291–10296, doi:10.1073/pnas.0804860105, 2008.

Table 1. Extinction (b_{ext}) and absorption (b_{abs}) coefficients and backscatter fraction (b) for the five mixing state representations. Radiative forcing efficiency (RFE) is calculated using Eq. (1).

	b_{ext} (Mm^{-1})	b_{abs} (Mm^{-1})	b	RFE ($W\,m^{-2}$)
INT-HOM	3.98	1.58	0.09	11.20
INT-COAT	3.63	1.53	0.16	9.11
EXT-BARE	3.43	0.56	0.11	−10.93
EXT-HOM	3.58	0.79	0.11	−5.46
EXT-COAT	3.51	0.75	0.11	−6.54

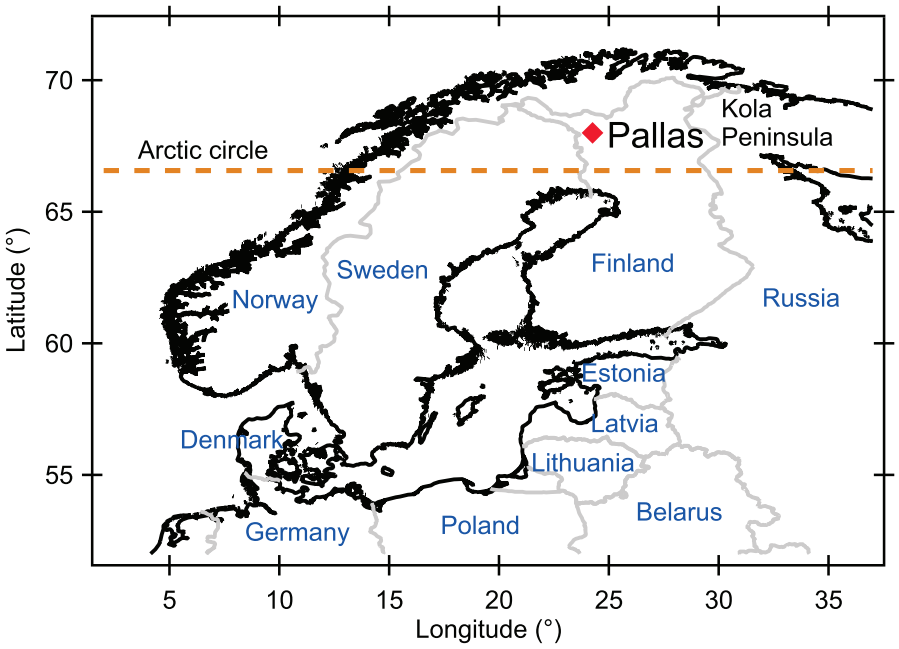

Figure 1. Location of the Pallas GAW station.

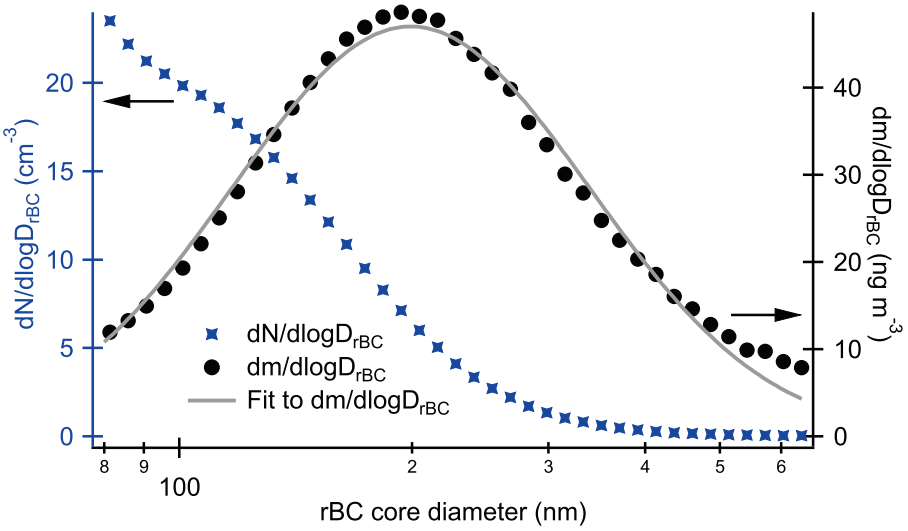

Figure 2. Campaign average rBC mass (black color, right axis) and number (blue color, left axis) size distributions. The solid gray line is a log-normal distribution fitted to the observations (geometric standard deviation is 1.70, geometric mean diameter is 199 nm and total area is 27 $\mathrm{ng\,m^{-3}}$).

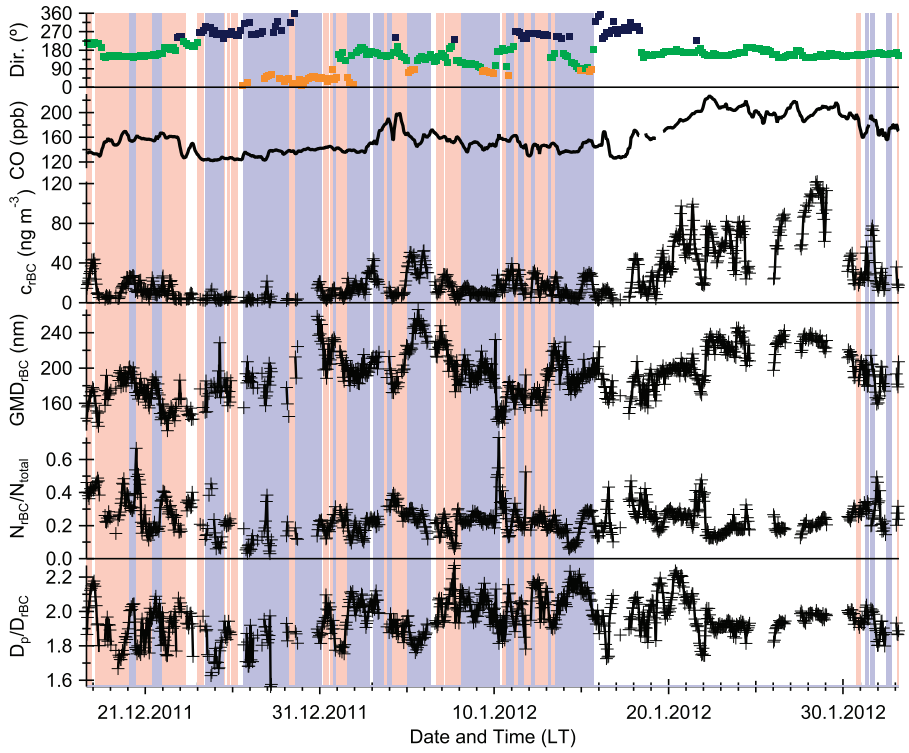

Figure 3. Time series of hourly averages of average trajectory direction (the color is based on three sectors: Arctic Ocean (orange) 0–90°, Continental Europe (green) 90–225° and North Atlantic (black) 225–360°), carbon monoxide (CO) concentration, total rBC mass concentration (c_{rBC}), geometric mass mean diameter (GMD_{rBC}), the fraction of 350–450 nm particles containing rBC (N_{rBC}/N_{total}), and ~~coated~~ particle to rBC core diameter ratio for 150–200 nm rBC cores (D_p/D_{rBC}). Blue background color indicates that the station was in cloud, red means no clouds and white means variable conditions or missing data.

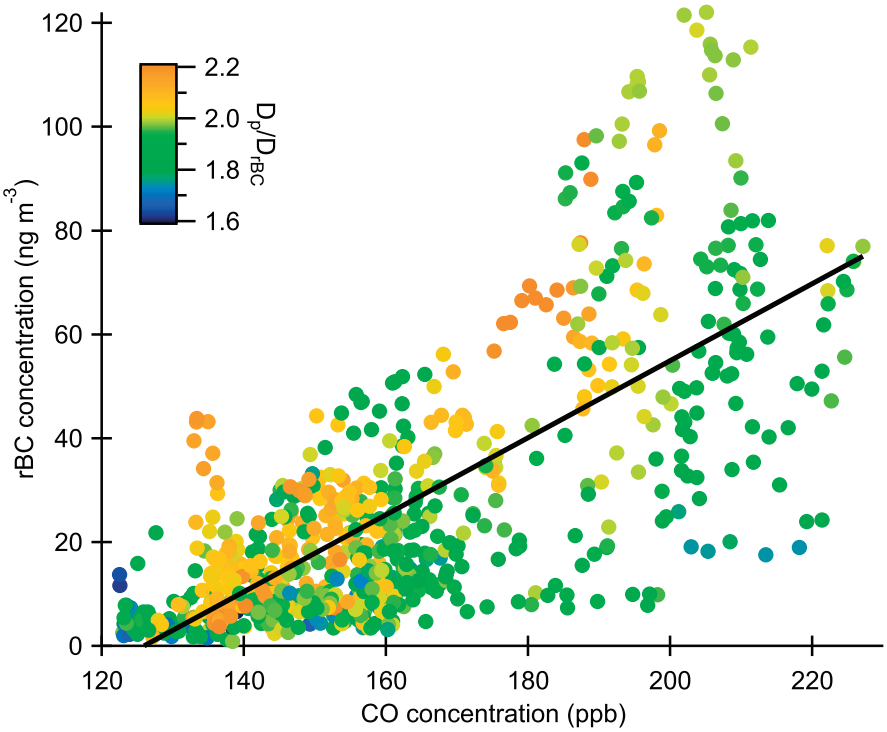

Figure 4. SP2 rBC mass concentration as a function of carbon monoxide (CO) concentration. Marker color shows the particle to rBC core diameter ratio for each data point. The solid black line shows the linear fit to the data.

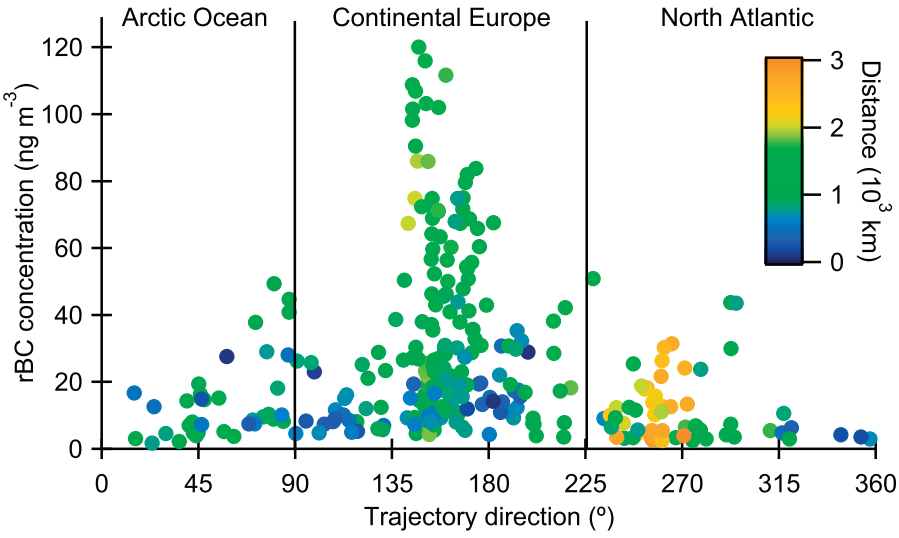

Figure 5. Total rBC mass concentration as a function of the average trajectory direction. Color scale indicates the average distance of the trajectory coordinate points from Pallas.

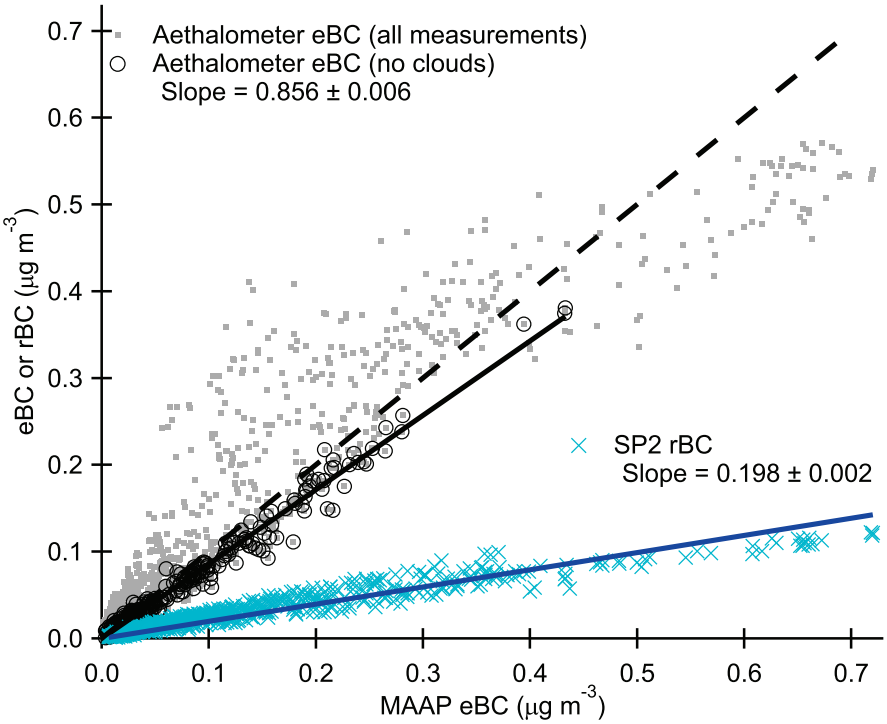

Figure 6. Aethalometer eBC (dots show all measurements and circles are those where the station is not in cloud) and SP2 rBC (crosses) as a function of MAAP eBC as well as linear fits (fixed zero offsets) to the data points. The dashed line shows 1 : 1 ~~correlation~~slope.

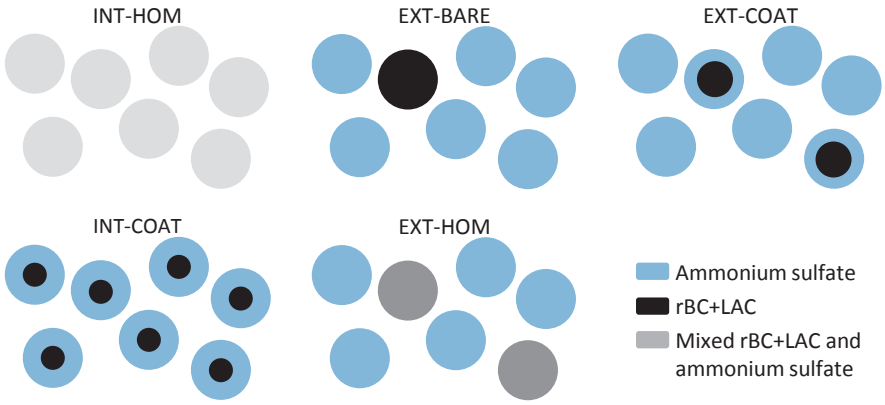

Figure 7. Illustration of the particle compositions for the five mixing state representations.